

Synthesis and Reactivity of Phosphine-Stabilized Phosphoranimine Cations, $[R_3P \cdot PR'_2=NSiMe_3]^+$

Keith Huynh,[‡] Alan J. Lough,[‡] Michelle A. M. Forgeron,[§] Martin Bendle,[†]
Alejandro Presa Soto,[†] Roderick E. Wasylishen,^{*,§,†} and Ian Manners^{*,†}

*School of Chemistry, University of Bristol, Bristol BS8 1TS, England, Davenport Laboratories,
Department of Chemistry, University of Toronto, 80 Saint George Street, Toronto, Ontario,
Canada M5S 3H6, and Gunning/Lemieux Chemistry Centre, University of Alberta,
Edmonton, Alberta, Canada T6G 2R3*

Received January 15, 2009; E-mail: roderick.wasylishen@ualberta.ca; ian.manners@bristol.ac.uk

Abstract: A series of phosphine-stabilized phosphoranimine cations $[R_3P \cdot PR'_2=NSiMe_3]^+$, which can be regarded as derivatives of the proposed transient reactive intermediate $[PR'_2=NSiMe_3]^+$ in the thermal condensation polymerization of phosphoranimines $(R''O)PR'_2=NSiMe_3$ to form poly(alkyl/arylphosphazenes) $[PR'_2=N]_n$ at 180–200 °C, have been prepared. The bromide salts $[R_3P \cdot PR'_2=NSiMe_3]Br$ [$R' = Me$ (**[6]**⁺), OCH_2CF_3 (**[8]**⁺); $R_3P = Me_3P$ (**(a)**), Et_3P (**(b)**), nBu_3P (**(c)**), *dmpm* (**(d)**, *dmpm* = dimethylphosphinomethane), *dmpe* (**(e)**, *dmpe* = dimethylphosphinoethane)] were prepared from the direct reactions between $BrMe_2P=NSiMe_3$ (**(5)**) and $Br(CF_3CH_2O)_2P=NSiMe_3$ (**(7)**) and the corresponding tertiary phosphines R_3P or the diphosphines $Me_2P(CH_2)_nPMe_2$ ($n = 1, 2$). Cations of the type **[6]**⁺ and **[8]**⁺, with electron-donating and -withdrawing groups at the phosphoranimine phosphorus center, respectively, undergo facile phosphine ligand substitution with the strong N-donor 4-dimethylaminopyridine (DMAP) to yield the corresponding DMAP-stabilized salts $[DMAP \cdot PR_2=NSiMe_3]Br$ [$R = Me$ (**[9]**⁺), OCH_2CF_3 (**[10]**⁺)]. Cations **[6]**⁺ with Br^- anions are particularly labile: for example, **[6a]Br** slowly releases PMe_3 , $BrSiMe_3$, and forms cyclic phosphazenes such as $[Me_2P=N]_4$. Anion exchange reactions between the salts **[6b]Br** or **[8c]Br** and $AgOTf$ ($OTf = CF_3SO_3$) quantitatively afforded the corresponding and more stable triflate salts **[6b]OTf** and **[8c]OTf**. Phosphine ligand abstraction reactions with $B(C_6F_5)_3$ were observed for the bromide salts **[6b]Br** and **[8c]Br**, which regenerated the phosphoranimines **(5)** and **(7)**, respectively, and formed the adduct $R_3P \cdot B(C_6F_5)_3$. In contrast, the triflate salts **[6b]OTf** and **[8c]OTf** were unreactive under the same conditions. X-ray structural analysis of the P-donor stabilized cations revealed longer P–P and P–N bond lengths and smaller P–N–Si bond angles for cations **[6]**⁺ compared to analogs **[8]**⁺. These structural differences were rationalized using the negative hyperconjugation bonding model. In addition, the $^1J_{PP}$ coupling constants for the cations **[6]**⁺ observed by both solution and solid-state ^{31}P NMR are remarkably small (13–25 Hz), whereas those for **[8]**⁺ are substantially larger and positive (276–324 Hz) and are as expected for $P(IV)^+–P(V)$ systems. DFT studies suggest that the significant difference in $^1J_{PP}$ couplings observed for **[6]**⁺ and **[8]**⁺ appears to be related to the electronegativity of the R' substituents at the phosphoranimine phosphorus center rather than the strength of the donor–acceptor P–P bond, which is slightly weaker in **[6]**⁺ relative to that in **[8]**⁺, as indicated by the X-ray data and reactivity studies.

Introduction

The study of phosphoranimines of general formula $R_3P=N–R'$ has been the subject of intense research over the past three decades.¹ Since their discovery by Staudinger and Meyer in 1919 from the reaction between tertiary phosphines R_3P and organic azides $R'N_3$,^{2a} many alternate preparative routes to phosphoranimines have been developed. Examples include the condensation reaction between dichlorotriorganophosphoranes and primary amines, known as the Kirsanov reaction,^{2b} and the

oxidative halogenation of *N*-silyl-substituted aminophosphines.^{2c} Interest in phosphoranimines originated from their ability to act as efficient synthons in imine transfer reactions with carbonyl-containing compounds through a process known as the aza-Wittig reaction.³

In addition to making a significant impact in synthetic organic chemistry, *N*-silylphosphoranimines have played important roles

[†] University of Bristol.

[‡] University of Toronto.

[§] University of Alberta.

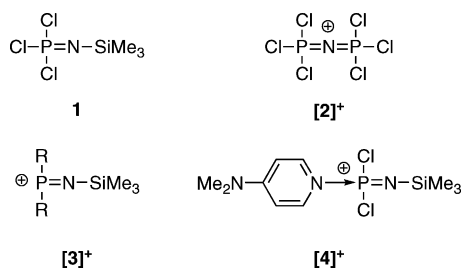
(1) Johnson, A. W. *Ylides and Imines of Phosphorus*; Wiley: New York, 1993.

(2) (a) Staudinger, H.; Meyer, J. *Helv. Chim. Acta* **1919**, *2*, 635. (b) Kirsanov, A. V. *Izv. Akad. Nauk SSSR* **1950**, 426. (c) Roesky, H. W.; Grimm, L. F. *Angew. Chem.* **1970**, *9*, 244.

(3) (a) Molina, P.; Vilaplana, M. L. *Synthesis* **1994**, 1197. (b) Bell, S. A.; Meyer, T. Y.; Geib, S. J. *J. Am. Chem. Soc.* **2002**, *124*, 10698. (c) Burland, M. C.; Meyer, T. Y. *Inorg. Chem.* **2003**, *42*, 3438.

(4) (a) Steiner, A.; Zacchini, S.; Richards, P. I. *Coord. Chem. Rev.* **2002**, *227*, 193. (b) Jäschke, B.; Jansen, M. *Z. Anorg. Allg. Chem.* **2002**, *628*, 2000. (c) Jäschke, B.; Jansen, M. *Z. Naturforsch. B: Chem. Sci.* **2002**, *57*, 1237. (d) Armstrong, A. F.; Chivers, T.; Krahn, M.; Parvez, M.; Schatte, G. *Chem. Commun.* **2002**, *20*, 2332. (e) Armstrong, A. F.; Chivers, T.; Tuononen, H. M.; Parvez, M.; Boeré, R. T. *Inorg. Chem.* **2005**, *44*, 7981.

in the development of molecular main group chemistry,⁴ coordination chemistry,⁵ catalysis,⁶ and inorganic polymer chemistry as precursors to polyphosphazenes.^{7–10} Routes to polyphosphazenes, from *N*-silylphosphoranimine monomers include thermal,⁸ fluoride-initiated,⁹ and more recently living cationic chain-growth condensation polymerization.¹⁰ Moreover, cationic phosphoranimine species have been implicated as key reactive intermediates in the polymerization mechanisms in several cases. For example, the ambient temperature polymerization of the phosphoranimine $\text{Cl}_3\text{P}=\text{NSiMe}_3$ (**1**),¹¹ which is catalyzed by PCl_5 , proceeds via the salt $[\text{Cl}_3\text{P}=\text{N}=\text{PCl}_3][\text{PCl}_6]$ (**[2]⁺PCl₆**).¹⁰ In addition, cationic *N*-silylphosphoranimines $[\text{R}_2\text{P}=\text{NSiMe}_3]^+$ (**[3]⁺**) are believed to be involved as highly reactive intermediates in the thermal condensation polymerization route to poly(alkyl/aryl)phosphazenes $[\text{PR}_2=\text{N}]_n$ from organophosphoranimines ($\text{R}'\text{O}$) $\text{PR}_2=\text{NSiMe}_3$ at 180–200 °C.^{8c} The highly Lewis acidic three-coordinate phosphorus(V) center present in cation **[3]⁺** is expected to be extremely reactive and would thus require stabilization from a neutral donor to render them isolable. Therefore, the isolation of donor-stabilized phosphoranimine cations could allow access to species that effectively model the polymerization intermediate **[3]⁺**. The previously reported¹² phosphoranimine cation $[\text{DMAP}\cdot\text{PCl}_2=\text{NSiMe}_3]^+$ (**[4]⁺**, DMAP = 4-dimethylaminopyridine) formed from the direct reaction between **1** and DMAP, is stabilized by the strong N-donor. However, in this case the donor ligand is strongly coordinated to the cationic phosphoranimine center, and therefore, limited reactivity was detected.



Efforts to diversify this chemistry by means of the formation of phosphoranimine cations bearing weaker non-nitrogen-based donors proceeded with reactions involving **1** and tertiary phosphines. However, we found that reactions between **1** and tertiary phosphines R_3P ($\text{R} = ^t\text{Bu}$ or Ph) yield the known

N-phosphinophosphoranimines $\text{R}_3\text{P}=\text{N}-\text{PCl}_2$ via a complex mechanism that involves a series of reductive dechlorination and condensation steps.¹³ These results indicated that the presence of a trichloro functionality at the phosphoranimine is incompatible with the preparation of the desired phosphine-stabilized phosphoranimine cations by this route. In this article, the successful synthesis and reactivity studies of the first examples of phosphine-stabilized phosphoranimine cations from the reaction of monohalogenophosphoranimines $\text{XR}_2\text{P}=\text{NSiMe}_3$ and tertiary phosphines are described in detail.¹⁴

Results and Discussion

Reactions between Bromophosphoranimines 5 and 7 and Tertiary Phosphines. In order to access the targeted phosphine-stabilized phosphoranimine cations the direct reactions between the bromophosphoranimines **5** and **7** and tertiary phosphines in CH_2Cl_2 or CHCl_3 were explored. Following treatment with Me_3P , Et_3P , or $^t\text{Bu}_3\text{P}$, the conversion of $\text{BrMe}_2\text{P}=\text{NSiMe}_3$ (**5**)¹⁵ [$\delta(^{31}\text{P}) = 10$ ppm] in moderate isolated yields to new products characterized by pairs of doublets was detected by $^{31}\text{P}\{^1\text{H}\}$ NMR spectroscopy. The $^1J_{\text{PP}}$ coupling constants observed for the products from the above reactions, between ± 13 and ± 25 Hz, were extremely small and the values are more typical of either two- or three-bond phosphorus–phosphorus coupling.¹⁶ Indeed, based on the small $^1J_{\text{PP}}$ couplings,¹⁷ we initially suspected that the targeted P–P coordination had not taken place. However, following workup and purification, single crystals of the products from the reactions between **5** and Me_3P and Et_3P were obtained and their solid-state structures were confirmed by single crystal X-ray diffraction. From these studies, the results of which will be discussed in detail later (see below), it was confirmed that P–P coordination had been successfully achieved from identification of the phosphine-stabilized phosphoranimine salts $[\text{Me}_3\text{P}\cdot\text{PMe}_2=\text{NSiMe}_3]\text{Br}$ (**[6a]Br**; Figure 1) and $[\text{Et}_3\text{P}\cdot\text{PMe}_2=\text{NSiMe}_3]\text{Br}$ (**[6b]Br**; Figure 2) in the solid state (Scheme 1).

The remarkably small $^1J_{\text{PP}}$ values measured for **[6a–c]Br** by ^{31}P NMR prompted an investigation into the preparation of other

- (5) Dehnicke, K.; Straehle, J. *Polyhedron* **1989**, *8*, 707.
 (6) Stephan, D. W. *Organometallics* **2005**, *24*, 2548.
 (7) Allcock, H. R. *Chemistry and Applications of Polyphosphazenes*; John Wiley and Sons: New York, 2003.
 (8) (a) Wisian-Neilson, P.; Neilson, R. H. *J. Am. Chem. Soc.* **1980**, *102*, 2848. (b) Neilson, R. H.; Hani, R.; Wisian-Neilson, P.; Meister, J. J.; Roy, A. K.; Hagnauer, G. L. *Macromolecules* **1987**, *20*, 910. (c) Neilson, R. H.; Wisian-Neilson, P. *Chem. Rev.* **1988**, *88*, 541. (d) Walker, C. H.; St. John, J. V.; Wisian-Neilson, P. *J. Am. Chem. Soc.* **2001**, *123*, 3846.
 (9) (a) Montague, R. A.; Matyjaszewski, K. *J. Am. Chem. Soc.* **1990**, *112*, 6721. (b) Matyjaszewski, K.; Moore, M. K.; White, M. L. *Macromolecules* **1993**, *26*, 6741.
 (10) (a) Honeyman, C. H.; Manners, I.; Morrissey, C. T.; Allcock, H. R. *J. Am. Chem. Soc.* **1995**, *117*, 7035. (b) Allcock, H. R.; Nelson, J. M.; Reeves, S. D.; Honeyman, C. H.; Manners, I. *Macromolecules* **1997**, *30*, 50. (c) Allcock, H. R.; Crane, C. A.; Morrissey, C. T.; Olshavsky, M. A. *Inorg. Chem.* **1999**, *38*, 280. (d) Allcock, H. R.; Reeves, S. D.; de Denu, C. R.; Crane, C. A. *Macromolecules* **2001**, *34*, 748. (e) Allcock, H. R.; Powell, E. S.; Maher, A. E.; Prange, R. L.; de Denu, C. R. *Macromolecules* **2004**, *37*, 3635. (f) Rivard, E.; Lough, A. J.; Manners, I. *Inorg. Chem.* **2004**, *43*, 2765. (g) Wang, B. *Macromolecules* **2005**, *38*, 643. (h) Blackstone, V.; Lough, A. J.; Murray, M.; Manners, I. *J. Am. Chem. Soc.* **2009**, *131*, 3658.

- (11) (a) Wang, B.; Rivard, E.; Manners, I. *Inorg. Chem.* **2002**, *41*, 1690. (b) For the first report of this species see Niecke, E.; Bitter, W. *Inorg. Nucl. Chem. Lett.* **1973**, *9*, 127.
 (12) (a) Rivard, E.; Huynh, K.; Lough, A. J.; Manners, I. *J. Am. Chem. Soc.* **2004**, *126*, 2286. (b) Huynh, K.; Rivard, E.; Lough, A. J.; Manners, I. *Chem.—Eur. J.* **2007**, *13*, 3431. (c) Huynh, K.; Rivard, E.; Lough, A. J.; Manners, I. *Inorg. Chem.* **2007**, *46*, 9979. (d) For examples of DMAP-stabilized cyclic phosphazene cations see Boomishankar, R.; Ledger, J.; Guilbaud, J.-B.; Campbell, N. L.; Bacsá, J.; Bonar-Law, R.; Khimiyak, Y. Z.; Steiner, A. *Chem. Commun.* **2007**, 5152.
 (13) Huynh, K.; Rivard, E.; LeBlanc, W.; Blackstone, V.; Lough, A. J.; Manners, I. *Inorg. Chem.* **2006**, *45*, 7922.
 (14) For a preliminary communication on some of this work see Huynh, K.; Lough, A. J.; Manners, I. *J. Am. Chem. Soc.* **2006**, *128*, 14002.
 (15) Wisian-Neilson, P.; Neilson, R. H. *Inorg. Chem.* **1980**, *19*, 1875.
 (16) (a) Dixon, K. R. In *Multinuclear NMR*; Mason, J., Ed.; Plenum Press: New York, 1987; pp 369–402. (b) Finer, E. G. and Harris, R. K., *Prog. Nucl. Magn. Reson. Spectrosc.*; Emsley, J. W., Feeney, J., Sutcliffe, L. H., Ed.; Pergamon Press: Elmsford, NY, 1971; Vol. 6, Chapter 2, pp 61–118. (c) Verkade, J. G.; Mosbo, J. A. In *Phosphorus-31 NMR Spectroscopy in Stereochemical Analysis*; Verkade, J. G., Quin, L. D., Eds.; VCH Publishers, Inc.: Deerfield Beach, FL, 1987; pp 425–463 (see pp 450–452). (d) Carpenter, Y.-Y.; Dyker, C. A.; Burford, N.; Lumsden, M. D.; Decken, A. *J. Am. Chem. Soc.* **2008**, *130*, 15732–15741. (e) Weigand, J. J.; Holthausen, M.; Fröhlich, R. *Angew. Chem., Int. Ed.* **2009**, *48*, 295.
 (17) The isolation of other P–P bonded compounds with unusually small $^1J_{\text{PP}}$ coupling constants have recently been reported. (a) Weigand, J. J.; Riegel, S. D.; Burford, N.; Decken, A. *J. Am. Chem. Soc.* **2007**, *129*, 7969. (b) Weigand, J. J.; Burford, N.; Mahnke, D.; Decken, A. *Inorg. Chem.* **2007**, *46*, 7689.

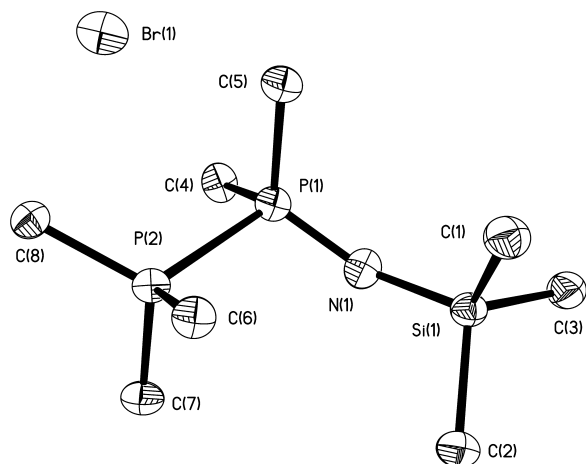


Figure 1. Molecular structure of **[6a]Br** with thermal ellipsoids at the 50% probability level. All hydrogen atoms have been omitted for clarity. Selected bond lengths [Å] and bond angles [deg]: P(1)–P(2) 2.2229(11), P(1)–N(1) 1.533(3), P(1)–C(4) 1.792(3), P(1)–C(5) 1.793(3), P(2)–C(6) 1.791(3), P(2)–C(7) 1.790(3), P(2)–C(8) 1.786(3), N(1)–Si(1) 1.696(3); P(2)–P(1)–N(1) 108.81(11), P(2)–P(1)–C(4) 102.41(11), P(2)–P(1)–C(5) 103.79(11), C(4)–P(1)–C(5) 106.65(15), C(4)–P(1)–N(1) 114.43(14), C(5)–P(1)–N(1) 118.99(15), P(1)–N(1)–Si(1) 143.98(16).

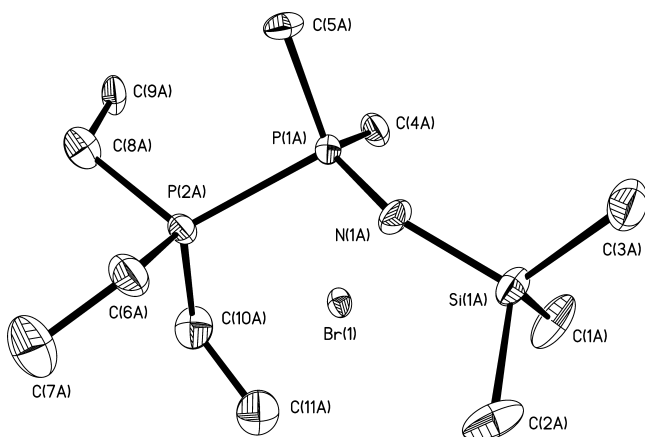
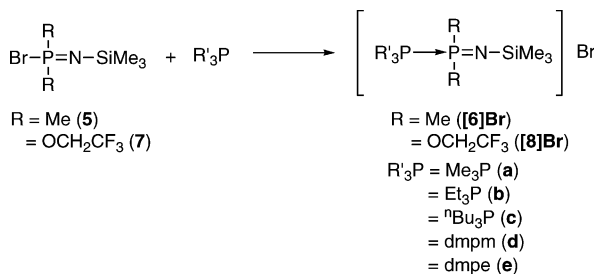


Figure 2. Molecular structure of **[6b]Br** with thermal ellipsoids at the 50% probability level. All hydrogen atoms have been omitted for clarity. Selected bond lengths [Å] and bond angles [deg]: P(1A)–P(2A) 2.217(3), P(1A)–N(1A) 1.520(5), P(1A)–C(4A) 1.821(6), P(1A)–C(5A) 1.802(6), P(2A)–C(6A) 1.858(8), P(2A)–C(8A) 1.856(6), P(2A)–C(10A) 1.748(7), N(1A)–Si(1A) 1.691(5); P(2A)–P(1A)–N(1A) 107.6(3), P(2A)–P(1A)–C(4A) 104.4(2), P(2A)–P(1A)–C(5A) 100.8(2), C(4A)–P(1A)–C(5A) 107.8(3), C(4A)–P(1A)–N(1A) 118.4(3), C(5A)–P(1A)–N(1A) 115.8(3), P(1A)–N(1A)–Si(1A) 145.0(4).

Scheme 1



phosphine-stabilized phosphoranimine cations in an effort to reveal a correlation between ¹J_{PP} and the phosphoranimine substituent, R. In similar reactions between the phosphoranimine Br(CF₃CH₂O)₂P=NSiMe₃ (**7**) [$\delta(^{31}\text{P}) = -34$ ppm]¹⁵ and the

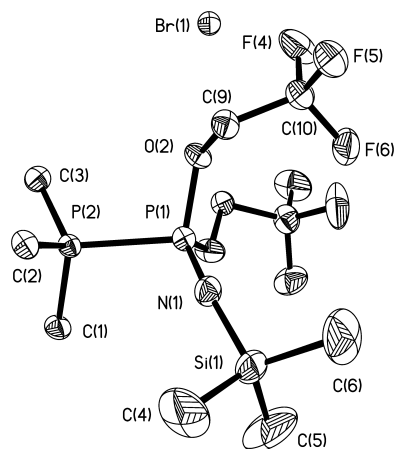


Figure 3. Molecular structure of **[8a]Br** with thermal ellipsoids at the 50% probability level. All hydrogen atoms have been omitted for clarity. Selected bond lengths [Å] and bond angles [deg]: P(1)–P(2) 2.1809(13), P(1)–N(1) 1.480(3), P(1)–O(1) 1.575(3), P(1)–O(2) 1.591(3), P(2)–C(1) 1.786(4), P(2)–C(2) 1.783(4), P(2)–C(3) 1.778(4), N(1)–Si(1) 1.694(4); P(2)–P(1)–N(1) 108.63(14), P(2)–P(1)–O(1) 103.12(12), P(2)–P(1)–O(2) 103.81(11), O(1)–P(1)–O(2) 102.99(14), O(1)–P(1)–N(1) 117.73(18), O(2)–P(1)–N(1) 118.69(18), P(1)–N(1)–Si(1) 161.0(3).

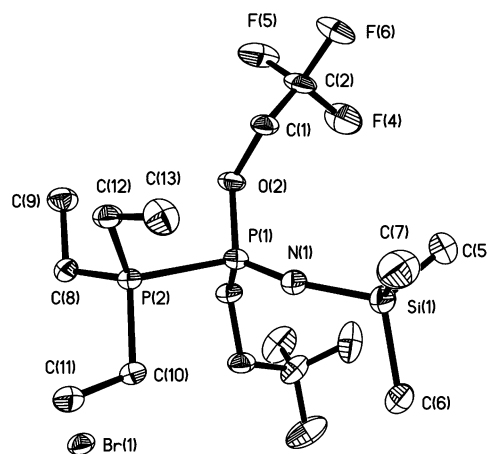
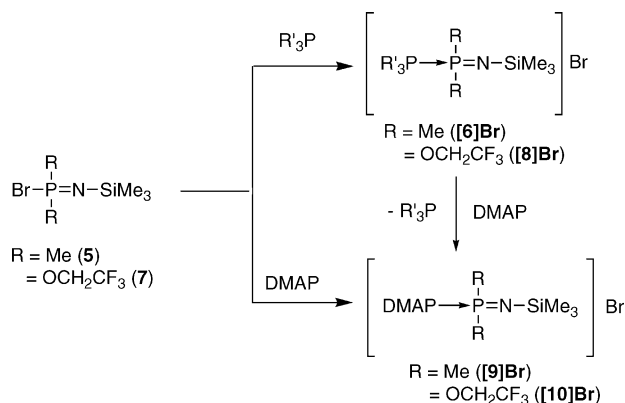


Figure 4. Molecular structure of **[8b]Br** with thermal ellipsoids at the 50% probability level. All hydrogen atoms have been omitted for clarity. Selected bond lengths [Å] and bond angles [deg]: P(1)–P(2) 2.2003(17), P(1)–N(1) 1.492(4), P(1)–O(1) 1.597(3), P(1)–O(2) 1.585(3), P(2)–C(8) 1.791(4), P(2)–C(10) 1.803(4), P(2)–C(12) 1.788(4), N(1)–Si(1) 1.722(4); P(2)–P(1)–N(1) 110.53(15), P(2)–P(1)–O(1) 102.09(13), P(2)–P(1)–O(2) 103.74(13), O(1)–P(1)–O(2) 97.21(16), O(1)–P(1)–N(1) 120.14(19), O(2)–P(1)–N(1) 120.43(19), P(1)–N(1)–Si(1) 158.0(3).

tertiary phosphines Me₃P, Et₃P, and ⁿBu₃P, the quantitative conversion of **7** to new products that exhibited pairs of doublets were observed in the ³¹P{¹H} NMR spectra. However, the magnitude of the ¹J_{PP} coupling constants for the target compounds **[8a–c]Br** (Scheme 1) were much larger, between ±277 and ±324 Hz, and were within the expected range of ¹J_{PP} values for P(IV)⁺–P(V) spin pairs compared to those observed for the analogous salts **[6a–c]Br**. After workup and purification, single crystals of **[8a]Br** (Figure 3) and **[8b]Br** (Figure 4) were also obtained and these were analyzed by single-crystal X-ray diffraction. This confirmed the generation of the phosphine-stabilized phosphoranimine salts [Me₃P•P(OCH₂CF₃)₂=NSiMe₃]Br (**[8a]Br**) and [Et₃P•P(OCH₂CF₃)₂=NSiMe₃]Br (**[8b]Br**) respectively. The much smaller ¹J_{PP} values for cations **[6]⁺** relative to **[8]⁺** appears to be related to the presence of electron-donating substituents at the phosphoranimine phos-

Scheme 2



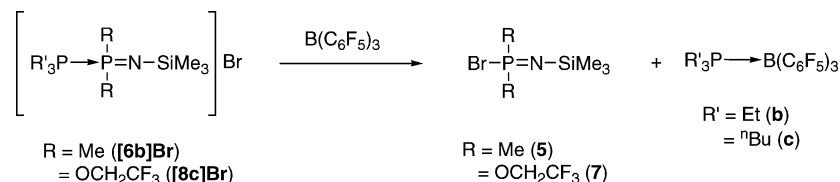
phorus center. We will return to this issue later after discussing their comparative chemistries, stabilities, and X-ray structural data in detail.

The surprisingly small $^1J_{\text{PP}}$ coupling constants observed for the cations $[\mathbf{6a-c}]^+$ are of the magnitude expected for two- or three-bond phosphorus–phosphorus couplings.¹⁶ Motivated by this observation, we proceeded to treat **5** with the bisphosphines dimethylphosphinomethane (dmpm) and dimethylphosphinoethane (dmpe), in an effort to deduce the $^2J_{\text{PP}}$ and $^3J_{\text{PP}}$ coupling constants for the cations $[\text{dmpm} \cdot \text{PMe}_2=\text{NSiMe}_3]^+$ ($[\mathbf{6d}]^+$) and $[\text{dmpe} \cdot \text{PMe}_2=\text{NSiMe}_3]^+$ ($[\mathbf{6e}]^+$), respectively. Interestingly, the $^2J_{\text{PP}}$ coupling constant for $[\mathbf{6d}]^+$ was observed to be ± 52 Hz, larger than the value for $^1J_{\text{PP}}$ (± 17 Hz). Similarly, the $^3J_{\text{PP}}$ coupling constant observed for $[\mathbf{6e}]^+$ was ± 30 Hz, while $^1J_{\text{PP}}$ was ± 23 Hz. Thus, the cations $[\mathbf{6d}]^+$ (Figure 5) and $[\mathbf{6e}]^+$ represent remarkable compounds that exhibit two- and three-bond phosphorus–phosphorus coupling constants that are greater than the corresponding $^1J_{\text{PP}}$ within the same compound.

For further comparison, we proceeded to prepare the analogous derivatives $[\text{dmpm} \cdot \text{P}(\text{OCH}_2\text{CF}_3)_2=\text{NSiMe}_3]\text{Br}$ ($[\mathbf{8d}]\text{Br}$) and $[\text{dmpe} \cdot \text{P}(\text{OCH}_2\text{CF}_3)_2=\text{NSiMe}_3]\text{Br}$ ($[\mathbf{8e}]\text{Br}$) from the reactions of **7** and the dmpm and dmpe bisphosphines. In contrast to the atypical P–P coupling constants revealed for $[\mathbf{6d}]^+$ and $[\mathbf{6e}]^+$, the coupling constants observed for $[\mathbf{8d}]^+$ ($^1J_{\text{PP}} = \pm 316$ Hz and $^2J_{\text{PP}} = \pm 64$ Hz) and $[\mathbf{8e}]^+$ ($^1J_{\text{PP}} = \pm 302$ Hz and $^3J_{\text{PP}} = \pm 34$ Hz) were within the range expected for typical one- and two-bond phosphorus–phosphorus coupling.

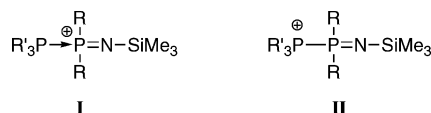
In order to further explore the scope of the chemistry, we also treated the phosphoranimines **5** and **7** with the less basic and more sterically encumbered tertiary phosphines PhMe_2P , Ph_2MeP , and Ph_3P . No reaction was observed with the exception of the partial (40%) conversion of **7** to $[\text{PhMe}_2\text{P} \cdot \text{P}(\text{OCH}_2\text{CF}_3)_2=\text{NSiMe}_3]\text{Br}$ ($[\mathbf{8f}]\text{Br}$) in the case of PhMe_2P . Moreover, a reaction was also not observed between the phosphoranimines **5** and **7** and the very sterically encumbered and strongly electron-donating phosphine $^t\text{Bu}_3\text{P}$. These results indicate that the formation of the P-donor stabilized cations $[\mathbf{6}]^+$ and $[\mathbf{8}]^+$ is strongly dependent on the steric demands of the tertiary phosphine. In addition, the partial reaction with PhMe_2P only in the case of **7** suggests an additional dependence on the

Scheme 3



nature of the phosphoranimine substituent where electron-withdrawing substituents at phosphorus enhance cation stability.

Ligand Substitution, Anion Exchange, and Relative Stability of Phosphine-Stabilized Phosphoranimine Cations $[\mathbf{6}]^+$ and $[\mathbf{8}]^+$. The unexpected large differences in observed $^1J_{\text{PP}}$ values for cations $[\mathbf{6}]^+$ and $[\mathbf{8}]^+$ prompted us to investigate and compare their relative reactivity. Two bonding models can be used to describe the cations $[\mathbf{6}]^+$ and $[\mathbf{8}]^+$: they can be represented as phosphine-stabilized phosphoranimine cations **I** or as phosphoranimine-substituted phosphonium cations **II**. Our initial reactivity studies involved attempted ligand substitution since the tertiary phosphine bound to the cationic phosphoranimine center would be expected to be labile if bonding model **I** is predominant.



The salts $[\text{Et}_3\text{P} \cdot \text{PMe}_2=\text{NSiMe}_3]\text{Br}$ ($[\mathbf{6b}]\text{Br}$) and $[\text{}^t\text{Bu}_3\text{P} \cdot \text{P}(\text{OCH}_2\text{CF}_3)_2=\text{NSiMe}_3]\text{Br}$ ($[\mathbf{8c}]\text{Br}$) exhibit enhanced solubility compared to analogues of type $[\mathbf{6}]\text{Br}$ and $[\mathbf{8}]\text{Br}$ and were thus chosen for the following reactivity studies. Upon treatment with the strong N-donor ligand DMAP, the quantitative conversion of $[\mathbf{6b}]\text{Br}$ and $[\mathbf{8c}]\text{Br}$ to the analogous DMAP-stabilized phosphoranimine salts $[\text{DMAP} \cdot \text{PMe}_2=\text{NSiMe}_3]\text{Br}$ ($[\mathbf{9}]\text{Br}$) and $[\text{DMAP} \cdot \text{P}(\text{OCH}_2\text{CF}_3)_2=\text{NSiMe}_3]\text{Br}$ ($[\mathbf{10}]\text{Br}$), respectively, was observed along with the concomitant release of the corresponding tertiary phosphine (Scheme 2). Alternatively, the salts $[\mathbf{9}]\text{Br}$ and $[\mathbf{10}]\text{Br}$ could be prepared from the direct reaction between DMAP and the phosphoranimines **5** and **7**, respectively.^{12a–c}

The salts $[\mathbf{6b}]\text{Br}$ and $[\mathbf{8c}]\text{Br}$ were also found to react quantitatively with the strong Lewis acid $\text{B}(\text{C}_6\text{F}_5)_3$ with phosphine abstraction from the P-donor-stabilized phosphoranimine cation to yield the corresponding phosphine–borane adduct $\text{R}'_3\text{P} \cdot \text{B}(\text{C}_6\text{F}_5)_3$, as shown by $^{31}\text{P}\{^1\text{H}\}$ and $^{11}\text{B}\{^1\text{H}\}$ NMR spectroscopy. Interestingly, during the reaction the cationic phosphoranimine fragment was found to recombine with the bromide anion to regenerate the corresponding bromophosphoranimine **5** and **7** (Scheme 3).

In order to gain further insight into this process, we attempted to replace the bromide counteranion in $[\mathbf{6b}]\text{Br}$ and $[\mathbf{8c}]\text{Br}$ by a less coordinating anion and to then induce the analogous phosphine-abstraction chemistry. Facile anion exchange was achieved when $[\mathbf{6b}]\text{Br}$ and $[\mathbf{8c}]\text{Br}$ were treated with AgOTf ($\text{OTf} = \text{triflate}, \text{CF}_3\text{SO}_3^-$) to yield the corresponding triflate salts $[\mathbf{6b}]\text{OTf}$ (Figure 6) or $[\mathbf{8c}]\text{OTf}$. It is also noteworthy that these reactions yielded AgBr as the exclusive byproduct and that no silver phosphine complexes were observed in solution due to a competitive ligand abstraction reaction (Scheme 4).

As the preparation of phosphine-stabilized phosphoranimine cations with a weakly coordinating anion (OTf) was possible, we treated $[\mathbf{6b}]\text{OTf}$ or $[\mathbf{8c}]\text{OTf}$ with the strong Lewis acid $\text{B}(\text{C}_6\text{F}_5)_3$ in an attempt to induce phosphine abstraction. If successful, isolation of either the salts $[\text{Me}_2\text{P}=\text{NSiMe}_3][\text{OTf}]$

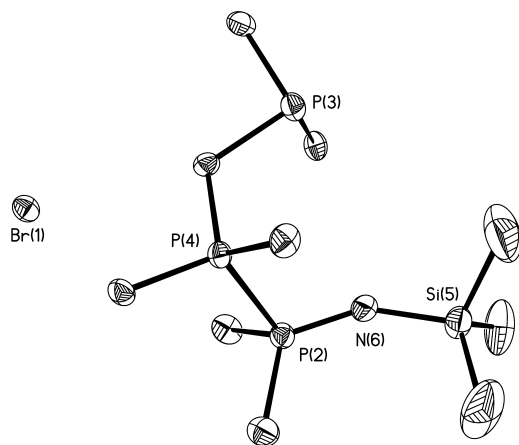


Figure 5. Molecular structure of **[6d]Br** with thermal ellipsoids at the 50% probability level. All hydrogen atoms have been omitted for clarity. Selected bond lengths [Å] and bond angles [deg]: P(2)–P(4) 2.215(3), P(2)–N(6) 1.537(7), P(2)–C(9) 1.803(7), P(2)–C(13) 1.794(8), N(6)–Si(5) 1.678(7); P(4)–P(2)–N(6) 108.1(3), P(4)–P(2)–C(9) 103.0(3), P(4)–P(2)–C(13) 102.0(3), C(9)–P(2)–C(13) 106.5(4), C(9)–P(2)–N(6) 119.3(4), C(13)–P(2)–N(6)–Si(5) 148.0(5).

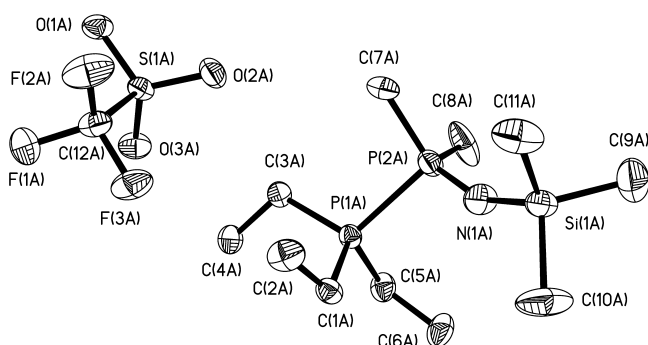
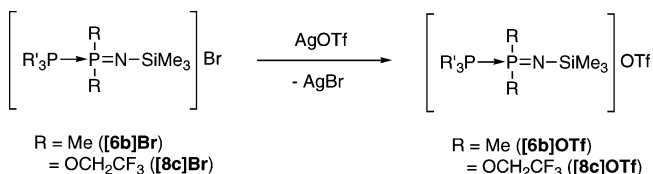


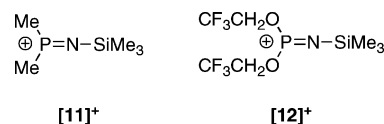
Figure 6. Molecular structure of **[6b]OTf** with thermal ellipsoids at the 50% probability level. All hydrogen atoms have been omitted for clarity. Selected bond lengths [Å] and bond angles [deg]: P(1A)–P(2A) 2.2280(12), P(2A)–N(1A) 1.508(3), P(2A)–C(7A) 1.776(4), P(2A)–C(8A) 1.794(5), P(1A)–C(1A) 1.794(3), P(1A)–C(3A) 1.795(4), P(1A)–C(5A) 1.798(4), N(1A)–Si(1A) 1.671(3); P(1A)–P(2A)–N(1A) 107.24(13), P(1A)–P(2A)–C(7A) 102.99(15), P(1A)–P(2A)–C(8A) 102.67(16), C(7A)–P(2A)–C(8A) 104.8(3), C(7A)–P(2A)–N(1A) 121.9(2), C(8A)–P(2A)–N(1A) 115.0(2), P(2A)–N(1A)–Si(1A) 154.0(2).

Scheme 4



(**[11]OTf**) and ((CF₃CH₂O)₂P=NSiMe₃)OTf (**[12]OTf**) or, more likely, the corresponding polar covalent molecular (triflate) phosphoranimines R₂(OSO₂CF₃)P=NSiMe₃ (R = Me or OCH₂CF₃) would illustrate an actual, or a potential route,¹⁸ respectively, to donor-free [R₂P=NSiMe₃]⁺ (**[3]**)⁺ cations, the aforementioned key proposed intermediate in the thermal condensation polymerization mechanism of alkyl/arylphosphoranimines.^{8c} However, when CDCl₃ solutions of either **[6b]OTf** or **[8c]OTf** were treated with equimolar amounts of B(C₆F₅)₃, no reaction was detected after 3 days. These results, combined with those in Scheme 3, unfortunately suggest that in order for the basic phosphine donor to be abstracted from the cations

[6b]⁺ and **[8c]⁺** by a strong Lewis acid, a nucleophilic anion, such as Br[−], must be present. These results suggest the possible existence of an equilibrium between the Br[−] salt of the phosphoranimine cation and the corresponding bromophosphoranimine and free phosphine in solution. This inspired additional studies.



More detailed studies of the stability of the cations **[6]⁺** and **[8]⁺** were therefore performed. The salt [Et₃P·PMe₂=NSiMe₃]Br (**[6b]Br**) was dissolved in CDCl₃ to give a dilute solution and subsequent analysis by ³¹P{¹H} NMR after 10 min showed three sets of signals, corresponding to a small amount of the starting salt **[6b]Br** [δ(³¹P) = 0.8 and 16 ppm, J_{PP} = ±24 Hz], together with 96% retroconversion to the bromophosphoranimine **5** [δ(³¹P) = 10 ppm] and free Et₃P [δ(³¹P) = −18 ppm]. These results provide clear support for an equilibrium process involving the dissociation of Et₃P and the coordination of the bromide anion to regenerate the bromophosphoranimine starting material **5**. In contrast to **[6b]Br**, the analogous triflate salt **[6b]OTf** exhibited indefinite stability in CDCl₃ solution at room temperature. The difference in stability between the bromide and triflate salts of **[6]⁺** in solution is likely due to the weaker ligating power of OTf[−] compared to Br[−].

The cations **[8]⁺** with trifluoroethoxy groups at phosphorus were also found to show slightly greater stability than the analogues **[6]⁺** with methyl substituents. The previously discussed observation that treatment of **7** with Me₂PhP yields **[8f]Br** with low conversion whereas no reaction was detected in the case of **5** is consistent with this assertion. Moreover, the salts **[8]Br** generally showed greater stability at room temperature than **[6]Br**. For example, when [Et₃P·P(OCH₂CF₃)₂=NSiMe₃]Br (**[8b]Br**) was dissolved in CDCl₃, no decomposition was observed by ³¹P{¹H} NMR after 10 min, which showed only resonances for the salt [δ(³¹P) = −19 and 27 ppm, J_{PP} = ±276 Hz]. However, after 24 h, small resonances for Br(CF₃CH₂O)₂P=NSiMe₃ [δ(³¹P) = −34 ppm] and Et₃P were clearly observable by ³¹P{¹H} NMR, increasing slowly in intensity to represent 11% retroconversion after 5 days. This suggests that, although **[8b]Br** also exists in equilibrium in solution, this salt is significantly more stable than **[6]Br**, which showed 96% retroconversion after 10 min under analogous conditions.

The low stability of the salts derived from **[6]⁺** with Br[−] as the counteranion was further emphasized by the observation that **[6a]Br**, with Me₃P coordinated to phosphorus, completely decomposed in CDCl₃ over 7 days at 25 °C. The growth of blocklike crystals of a new product was detected and these were identified by a single-crystal X-ray diffraction study as the cyclic tetraphosphazene [Me₂P=N]₄ (**13**) (Figure 7).¹⁹ Analysis of the mother liquor by ¹H and ³¹P{¹H} NMR spectroscopy revealed the presence of the decomposition byproducts BrSiMe₃ and free Me₃P, in addition to the cyclic phosphazene rings [Me₂P=N]_x (x = 3, 4, and 5).¹⁵ After solvent evaporation, electron impact

(18) The formation of the polar covalent molecular (triflate)phosphoranimines R₂(CF₃O₂SO)P=NSiMe₃ (R = Me or OCH₂CF₃) would suggest that the use of more weakly coordinating anions (e.g., [B(C₆F₅)₄][−] or [carborane][−]) might allow “free” cations **[11]⁺** and **[12]⁺** to be prepared.

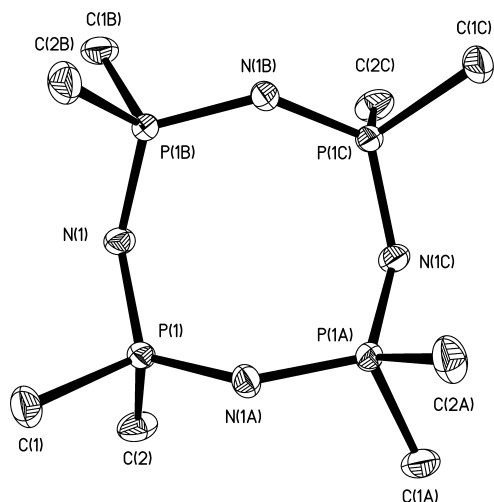


Figure 7. Molecular structure of **13** with thermal ellipsoids at the 50% probability level. All hydrogen atoms have been omitted for clarity. Selected bond lengths [Å] and bond angles [deg]: P(1)–N(1) 1.5937(17), P(1)–N(1A) 1.5917(17), P(1)–C(1) 1.794(2), P(1)–C(2) 1.796(2); N(1)–P(1)–N(1A) 119.90(12), N(1)–P(1)–C(1) 110.12(10), N(1)–P(1)–C(2) 104.46, N(1A)–P(1)–C(1) 104.75(10), N(1A)–P(1)–C(2) 112.53(10), C(1)–P(1)–C(2) 104.08(12), P(1)–N(1)–P(1A) 132.16(11).

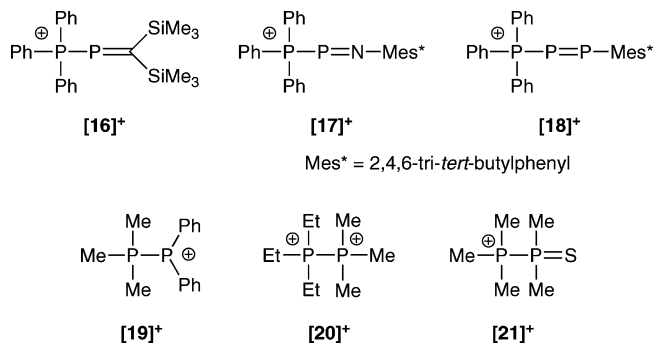
Table 1. Selected Bond Lengths and Angles for **[6]⁺**, **[8]⁺**, **[9]⁺**, **[10]⁺**, and Related Compounds **[16]⁺**–**[21]⁺**

	P–P [Å]	P–N [Å]	P–N(3)–E [deg]
[6a]Br	2.2229(11)	1.533(3)	143.98(16) (E = Si)
[6b]Br	2.217(3)	1.520(5)	145.0(4) (E = Si)
[6b]OTf	2.2280(12)	1.508(3)	154.0(2) (E = Si)
[6d]Br	2.215(3)	1.537(7)	148.0(5) (E = Si)
[8a]Br	2.1809(13)	1.480(3)	161.0(3) (E = Si)
[8b]Br	2.2003(17)	1.492(4)	158.0(3) (E = Si)
[9]Br^{12b}	–	1.526(2)	141.74(13) (E = Si)
[10]Br^{12b}	–	1.476(3)	166.7(2) (E = Si)
[16]AlCl₄²¹	2.267(2)	–	–
[17]OTf²²	2.625(2)	1.486(4)	169.5(4) (E = C)
[18]BPh₄²³	2.206(1)	–	–
[19]OTf^{24b}	2.187(2)	–	–
[20]OTf^{17a}	2.198(2)	–	–
[21]OTf^{17b}	2.206(1)	–	–

mass spectrometry also revealed the presence of the cyclic hexamer $[\text{Me}_2\text{P}=\text{N}]_6$ and heptamer $[\text{Me}_2\text{P}=\text{N}]_7$.¹⁵

Structures of, and Bonding in, Phosphine-Stabilized Phosphoranimine Cations. Views of the formula units for **[6a]Br**, **[6b]Br**, **[8a]Br**, **[8b]Br**, **[6d]Br**, and **[6b]OTf** determined by single-crystal X-ray diffraction are shown in Figures 1–6. Selected bond lengths and angles for the phosphoranimine salts are given in Table 1 along with structural data of related compounds for comparison. The P–P coordination bonds for the cations **[6]⁺** and **[8]⁺** range from 2.1809(13) to 2.2280(12) Å and show small deviations from the average P–P single bond length of 2.20 Å.²⁰ In particular, the P–P bond lengths found in **[6]⁺** and **[8]⁺** are in fairly close agreement with those for the analogous cationic species **[16]⁺** and **[18]⁺**–**[21]⁺** whereas that present in **[17]⁺** is significantly longer.

A slight difference in P–P bond lengths for **[6]⁺** and **[8]⁺** can be observed. The P–P bond lengths for cations **[8]⁺**, where



electron-withdrawing substituents are present on the phosphoranimine, are slightly (ca. 0.02 Å) shorter than those observed in **[6]⁺**, which possesses electron-donating groups. Moreover, striking differences are observed in the phosphorus–nitrogen bond lengths and in the internal phosphoranimine nitrogen bond angles found for **[6]⁺** and **[8]⁺**. A range of 1.508(3)–1.537(7) Å is found for the phosphorus–nitrogen double bonds in the **[6]⁺** cations, which is slightly shorter than the typical P=N bond range of 1.54–1.58 Å.²⁵ However, significantly shorter phosphorus–nitrogen bonds are observed for the cations **[8a]⁺** and **[8b]⁺**, 1.480(3) and 1.492(4) Å, respectively, and these values approach the P–N bond length of 1.475(8) Å found in the phosphoradiazonium cation $[\text{P}=\text{N}(\text{Mes}^*)]^+$ (Mes* = 2,4,6-tri-*tert*-butylphenyl),²⁶ where a formal triple bond exists between phosphorus and nitrogen. In addition, the P–N–Si bond angles found in **[8]⁺**, 158.0(3)° and 161.0(3)°, are considerably larger than those found in **[6]⁺**, between 143.98(16)° and 151.9(2)°.

Parallel differences in structural parameters for the DMAP-stabilized cations **[9]⁺** and **[10]⁺** are also observed. The cation **[10]⁺**, with electron-withdrawing trifluoroethoxy groups at phosphorus, exhibits a significantly shorter (DMAP)N–P and P–N(Si) bond length and a wider P–N–Si bond angle (values 1.724(3) Å, 1.476(3) Å, and 166.7(2)°, respectively) compared to **[9]⁺**, with methyl substituents (values 1.7946(19) Å, 1.526(2) Å, and 141.74(13)°, respectively). Significantly, the salts **[6a]Br** and **[9]Br** exhibit very similar phosphoranimine P–N bond lengths and P–N–Si bond angles and yet bear entirely different donor ligands.²⁷ Corresponding structural similarities are also noted for the salts **[8a]Br** and **[10]Br**. The structural comparisons between the salts **[6a]Br** and **[9]Br**, in addition to **[8a]Br** and **[10]Br**, clearly illustrate the key influence of the phosphoranimine substituents on the P–N lengths and P–N–Si bond

(19) The formation of **13** from the decomposition of **5** at ambient temperature is highly unlikely. Neat samples of **5** have been heated at 120 °C for 3 h and no decomposition was observed.¹⁵ The formation of **13** from **5** only occurred when **5** was heated neat at 250 °C for 26 h. For the first structural report of **13** see Dougill, M. W. *J. Chem. Soc.* **1961**, 5471.

(20) (a) Gilheany, D. G. In *The Chemistry of Organophosphorus Compounds*; Hartley, F. R., Ed.; John Wiley and Sons: New York, 1990; Vol. 1, Chapter 2. (b) Wells, A. F., *Structural Inorganic Chemistry*, 5th ed.; Oxford University Press: New York, 1984.

(21) David, G.; Niecke, E.; Nieger, M.; Radseck, J.; Schoeller, W. W. *J. Am. Chem. Soc.* **1994**, *116*, 2191.

(22) Burford, N.; Cameron, T. S.; Clyburne, J. A. C.; Eichele, K.; Robertson, K. N.; Sereda, S.; Wasylishen, R. E.; Whittle, W. A. *Inorg. Chem.* **1996**, *35*, 5460.

(23) Romanenko, V. D.; Rudzevich, V. L.; Rusanov, E. B.; Chernega, A. N.; Senio, A.; Sotiropoulos, J. M.; Pfister-Guillouzo, G.; Sanchez, M. *Chem. Commun.* **1995**, 1383.

(24) (a) Burford, N.; Cameron, T. S.; Ragogna, P. J.; Ocando-Mavarez, E.; Gee, M.; McDonald, R.; Wasylishen, R. E. *J. Am. Chem. Soc.* **2001**, *123*, 7947. (b) Burford, N.; Ragogna, P. J.; McDonald, R.; Ferguson, M. *J. Am. Chem. Soc.* **2003**, *125*, 14404.

(25) Allen, C. W. *Coord. Chem. Rev.* **1994**, *130*, 137.

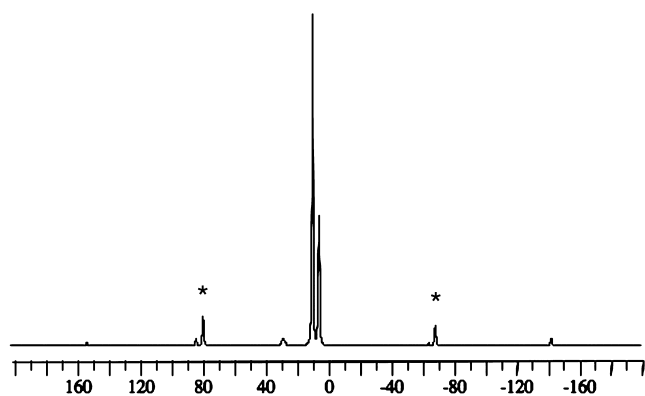
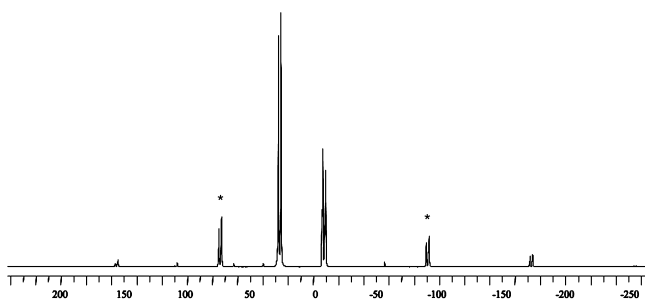
(26) Niecke, E.; Nieger, M.; Reichert, F. *Angew. Chem., Int. Ed. Engl.* **1988**, *27*, 1715.

(27) pK_a 's for $[\text{DMAPH}]^+$ and $[\text{Me}_3\text{PH}]^+$ are 9.2 and 8.65 respectively; see: (a) Bordwell, F. G. *Acc. Chem. Res.* **1988**, *21*, 456. (b) Henderson, Jr., W. A.; Streuli, C. A. *J. Am. Chem. Soc.* **1960**, *82*, 5791.

Table 2. $^{31}\text{P}\{^1\text{H}\}$ NMR Data for Derivatives of the Cations $[\mathbf{6}]^+$ and $[\mathbf{8}]^+$

	δ (ppm)		$J_{\text{PP}}^{a,b,c}$ (Hz)	
	solution ^d	CP-MAS	solution ^d	CP-MAS
[6a]Br	2.8	8.4	13.0 ^a	14 ^a
	-1.4	4.3		
[6b]Br	16.7	17.8	24.6 ^a	^e
	0.8	4.4		
[6c]Br	8.4	^f	22.8 ^a	^f
	-1.1			
[6d]Br	10.8	^f	17.0 ^a	^f
	6.7		51.6 ^b	
[6e]Br	-47.9			
	9.1	8.9	20.2 ^a	22 ^a
[8a]Br	3.3	-4.1	25.1 ^c	32 ^c
	-42.5	-46.2		
[8b]Br	11.9	11.1	324.0 ^a	322 ^a
	-15.6	-16.4		
[8c]Br	27.5	26.6	276.0 ^a	262 ^a
	-19.3	-8.6		
[8d]Br	22.2	^f	277.9 ^a	^f
	-18.5			
[8e]Br	16.9	^f	316.2 ^a	^f
	-15.2		63.6 ^b	
[8e]Br	-49.1			
	18.1	^f	302.4 ^a	^f
[8e]Br	-15.1		33.8 ^c	
	-42.6			

^a $^1J_{\text{PP}}$. ^b $^2J_{\text{PP}}$. ^c $^3J_{\text{PP}}$. ^d 25 °C (CDCl₃). ^e Not resolved. ^f Not measured.

**Figure 8.** Solid-state $^{31}\text{P}\{^1\text{H}\}$ CP-MAS NMR spectrum of $[\mathbf{6a}]\text{Br}$ acquired at a frequency of 121.60 MHz. A rotor spinning speed of 9.0 kHz was used; spinning side bands are indicated by asterisks.**Figure 9.** Solid-state $^{31}\text{P}\{^1\text{H}\}$ CP-MAS NMR spectrum of $[\mathbf{8b}]\text{Br}$ acquired at a frequency of 121.60 MHz. A rotor spinning speed of 10.0 kHz was used; spinning side bands are indicated by asterisks.

although anion-dependent retroconversion to $\mathbf{5}$ and PR_3 can occur as described earlier. In addition, the solid-state ^{31}P NMR data indicated that solvation effects on the ^{31}P chemical shifts and $^1J_{\text{PP}}$ values for $[\mathbf{6}]^+$ and $[\mathbf{8}]^+$ are negligible. The large difference in observed $^1J_{\text{PP}}$ values reinforces the fact that $^1J_{\text{PP}}$

is incredibly sensitive to structural changes; however, given that $^1J_{\text{PP}}$ values can be positive or negative, it is not surprising that there are molecules exhibiting small $^1J_{\text{PP}}$ values. Clearly, cations $[\mathbf{6}]^+$ fall into this category. It is important to recognize that a precise description of the dependence of $^1J_{\text{PP}}$ on the nature of the P–P bond is complicated and cannot be rationalized simply in terms of bond order, bond length, or bond strength arguments;^{32b,35} nevertheless, current computational quantum chemistry methods are capable of reproducing experimental trends in this important structural parameter and may be used to provide insight into observed J_{PP} values.

Summary

Donor-stabilized phosphoranimine cations $[\text{L}\cdot\text{PR}'_2=\text{NSiMe}_3]^+$ represent derivatives of the proposed reactive cationic intermediate $[\text{PR}'_2=\text{NSiMe}_3]^+$ in the thermal condensation polymerization of phosphoranimines to afford poly(alkyl/arylphosphazenes). Examples with P-donor coordination were prepared by the direct reactions between bromophosphoranimines $\text{BrMe}_2\text{P}=\text{NSiMe}_3$ ($\mathbf{5}$) and $\text{Br}(\text{CF}_3\text{CH}_2\text{O})_2\text{P}=\text{NSiMe}_3$ ($\mathbf{7}$) and tertiary phosphines. In the resulting bromide salts of the phosphine-stabilized phosphoranimine cations $[\mathbf{6}]^+$ and $[\mathbf{8}]^+$ the P-donor is weakly bound to the phosphoranimine moiety and can be readily displaced by stronger donors such as DMAP or abstracted by the strong Lewis acid $\text{B}(\text{C}_6\text{F}_5)_3$. Moreover, the retroconversion of the bromide salts of $[\mathbf{6}]^+$ and, to a lesser extent $[\mathbf{8}]^+$, in solution to the bromophosphoranimines $\mathbf{5}$ and $\mathbf{7}$, respectively, further supports the presence of weak phosphine coordination.

The magnitude of the $^1J_{\text{PP}}$ coupling constant is much smaller for the cations $[\mathbf{6}]^+$ compared to $[\mathbf{8}]^+$ in both solution and in the solid state due to the increased electronegativity of the phosphoranimine substituents. The P–P donor–acceptor bond in cations $[\mathbf{6}]^+$ is slightly longer and apparently weaker than in the analogues $[\mathbf{8}]^+$ based on X-ray diffraction and stability studies. However, the relative strengths of the donor–acceptor P–P interaction are unlikely to explain the substantial difference in $^1J_{\text{PP}}$ values.

Phosphine coordination appears to be particularly weak in the case of cations $[\mathbf{6}]^+$. The potential relevance of such species as models for the proposed cationic polymerization intermediate $[\text{PR}'_2=\text{NSiMe}_3]^+$ is underscored by the ambient temperature decomposition of $[\mathbf{6a}]\text{Br}$ to cyclic phosphazenes oligomers $[\text{Me}_2\text{PN}]_x$. Further investigations and extensions to even weaker phosphorus donors such as phosphites are underway with the aim of developing an ambient temperature route to linear poly(alkyl/aryl)phosphazenes rather than cyclic oligomers.¹⁴

Experimental Section

Materials and Instrumentation. All reactions and manipulations were carried out under an atmosphere of prepurified nitrogen or argon (Air Products) using common Schlenk techniques or an inert atmosphere glovebox (M-Braun). Hexanes were dried and collected using a Grubbs-type solvent purification system manufactured by M-Braun. CHCl_3 and CH_3CN were dried at reflux over CaH_2 . Et_2O was dried at reflux over $\text{Na}/\text{benzophenone}$. Solid-state $^1\text{H} \rightarrow ^{31}\text{P}$ cross-polarization magic-angle spinning (CP-MAS) $^{31}\text{P}\{^1\text{H}\}$ NMR spectra were recorded on a Bruker Avance spectrometer operating at a frequency of 121.59 MHz ($B_0 = 7.05$ T) and using spinning speeds of $\nu_{\text{rot}} =$

(35) Vaara, J.; Jokisaari, J.; Wasylishen, R. E.; Bryce, D. L. *Prog. Nucl. Magn. Reson. Spectrosc.* **2002**, *41*, 233.

Table 3. Crystal Data and Structure Refinement for [6a]Br, [6b]Br, [6b]OTf, and [6d]Br

	[6a]Br	[6b]Br	[6b]OTf	[6d]Br
empirical formula	C ₈ H ₂₄ BrNP ₂ Si	C ₁₁ H ₃₀ BrNP ₂ Si	C ₁₂ H ₃₀ F ₃ NO ₃ P ₂ SSi	C ₁₀ H ₂₉ BrNP ₂ Si
formula weight	304.22	346.30	415.46	364.25
crystal system	orthorhombic	triclinic	orthorhombic	monoclinic
space group	<i>Pbca</i>	<i>P</i> $\bar{1}$	<i>Pbca</i>	<i>P2</i> ₁ / <i>c</i>
<i>a</i> (Å)	11.7432(2)	14.0798(7)	12.4326(2)	14.9772(8)
<i>b</i> (Å)	11.5531(4)	17.0889(8)	28.4196(7)	10.9378(4)
<i>c</i> (Å)	22.8714(9)	18.0705(6)	36.7682(9)	11.6076(11)
α (°)	90	118.170(2)	90	90
β (°)	90	104.297(3)	90	102.029(2)
γ (°)	90	90.164(2)	90	90
<i>V</i> (Å ³)	3102.97(17)	3677.7(3)	12991.3(5)	1859.8(2)
<i>Z</i>	8	8	24	4
<i>D</i> _c (mg m ⁻³)	1.302	1.251	1.274	1.301
μ (Mo K α), mm ⁻¹	2.902	2.457	0.386	2.505
<i>F</i> (000)	1264	1456	5280	760
θ range (°)	2.63–27.46	2.67–27.54	2.64–25.04	2.59–25.00
index ranges	–15 ≤ <i>h</i> ≤ 15 –14 ≤ <i>k</i> ≤ 14 –29 ≤ <i>l</i> ≤ 29	–18 ≤ <i>h</i> ≤ 18 –22 ≤ <i>k</i> ≤ 19 –23 ≤ <i>l</i> ≤ 23	–14 ≤ <i>h</i> ≤ 14 –32 ≤ <i>k</i> ≤ 33 –43 ≤ <i>l</i> ≤ 43	–17 ≤ <i>h</i> ≤ 17 –12 ≤ <i>k</i> ≤ 12 –13 ≤ <i>l</i> ≤ 13
reflins colld	23 642	42 338	58 490	3258
independent	3544	42 338	11 447	3258
temp (K)	150(2)	150(1)	150(2)	150(1)
GOF on <i>F</i> ²	1.024	1.029	1.014	1.074
<i>R</i> , % (<i>I</i> > 2 σ [<i>I</i>]) ^a	3.95	6.84	5.30	6.53
<i>R</i> _w , % ^b	9.83	18.65	13.03	19.62
peak/hole (e/Å ³)	0.441/–0.460	0.865/–1.174	0.364/–0.305	0.957/–0.486

$$^a R = \sum |F_o| - |F_c| / \sum |F_o|. \quad ^b R_w = \{ \sum [w(F_o^2 - F_c^2)^2] / \sum [w(F_o^2)] \}^{1/2}.$$

4.0–10.0 kHz. Ammonium dihydrogen phosphate (ADP) was used for ³¹P chemical shift referencing with $\delta(^{31}\text{P}) = 0.81$ ppm and pulse width calibration ($\pi/2 = 4.00$ μs). Samples were powdered and packed in 4.0 mm outer diameter ZrO₂ rotors in an argon-filled glovebox. Sweep widths of 60–100 kHz, acquisition times of 50–70 ms, pulse delays of 5.0 s, and contact times of 4.5–6.0 ms were employed to record 512–2k scans. ¹H, ¹³C{¹H}, ¹⁹F, ¹¹B, and ³¹P{¹H} solution NMR spectra were obtained on a Varian Gemini 300 spectrometer (300.1, 75.4, 282.3, 96.3, and 121.5 MHz, respectively) and were referenced either to protic impurities in the solvent (¹H) or externally to SiMe₄ (¹³C{¹H}), CFCl₃ (¹⁹F) in CDCl₃, BF₃·Et₂O (¹¹B), and 85% H₃PO₄ (³¹P{¹H}) in CDCl₃. Elemental analyses were performed at the University of Toronto using a Perkin-Elmer 2400 Series CHN analyzer. Despite numerous attempts, accurate analyses could not be obtained for the labile phosphine-stabilized cation salts. Me₃P (1 M in toluene), Et₃P, ⁿBu₃P, Me₂PhP, dmpm, dmpe, DMAP, AgOTf, and B(C₆F₅)₃ were purchased from Aldrich and used as received. BrMe₂P=NSiMe₃ (**5**)¹⁵ and Br(CF₃CH₂O)₂P=NSiMe₃ (**7**)¹⁵ were prepared according to literature procedures.

Crystallographic Structure Determination. Data were collected on a Nonius Kappa-CCD diffractometer using graphite-monochromated Mo K α radiation ($\lambda = 0.71073$ Å). A combination of $1^\circ \phi$ and ω (with κ offsets) scans were used to collect sufficient data. The data frames were integrated and scaled using the Denzo-SMN package.³⁶ The structures were solved and refined with the SHELXTL-PC v6.12 software package.³⁷ Refinement was carried out by full-matrix least-squares on *F*² using data (including negative intensities) with hydrogen atoms bonded to carbon atoms included in calculated positions and treated as riding atoms (data in Tables 3 and 4).

¹J_{PP} Calculations. Nonrelativistic zeroth-order regular approximation density functional theory (ZORA DFT)³⁸ calculations of ¹J_{PP} were performed on the isolated cations, [6a]⁺ and [8a]⁺, using the CPL module³⁹ of the Amsterdam Density Functional

Table 4. Crystal Data and Structure Refinement for [8a]Br, [8b]Br, and 13

	[8a]Br	[8b]Br	13
empirical formula	C ₁₀ H ₂₂ BrF ₆ NO ₂ P ₂ Si	C ₁₃ H ₂₈ BrF ₆ NO ₂ P ₂ Si	C ₈ H ₂₄ N ₄ P ₄
formula weight	472.23	514.30	300.19
crystal system	monoclinic	monoclinic	tetragonal
space group	<i>P2</i> ₁ / <i>c</i>	<i>P2</i> ₁ / <i>c</i>	<i>I4</i> ₁ / <i>a</i>
<i>a</i> (Å)	16.0802(5)	17.6985(16)	15.7111(8)
<i>b</i> (Å)	9.2065(3)	7.5122(4)	15.7111(8)
<i>c</i> (Å)	15.4421(3)	17.6621(15)	6.4101(4)
α (°)	90	90	90
β (°)	111.208(2)	93.383(3)	90
γ (°)	90	90	90
<i>V</i> (Å ³)	2131.26(10)	2344.2(3)	1582.26(15)
<i>Z</i>	4	4	4
<i>D</i> _c (mg m ⁻³)	1.472	1.457	1.260
μ (Mo K α), mm ⁻¹	2.187	1.995	0.461
<i>F</i> (000)	952	1048	640
θ range (°)	2.60–27.49	2.64–27.46	2.59–27.45
index ranges	–18 ≤ <i>h</i> ≤ 19 –11 ≤ <i>k</i> ≤ 11 –19 ≤ <i>l</i> ≤ 18	–22 ≤ <i>h</i> ≤ 22 –9 ≤ <i>k</i> ≤ 9 –22 ≤ <i>l</i> ≤ 22	–15 ≤ <i>h</i> ≤ 20 –20 ≤ <i>k</i> ≤ 20 –8 ≤ <i>l</i> ≤ 8
reflins colld	13 292	12 430	3062
independent	4666	5236	898
temp (K)	150(2)	150(1)	150(2)
GOF on <i>F</i> ²	1.070	0.944	1.070
<i>R</i> , % (<i>I</i> > 2 σ [<i>I</i>]) ^a	4.36	5.50	3.54
<i>R</i> _w , % ^b	12.84	13.65	8.75
peak/hole (e/Å ³)	0.800/–0.659	0.643/–0.643	0.253/–0.326

$$^a R = \sum |F_o| - |F_c| / \sum |F_o|. \quad ^b R_w = \{ \sum [w(F_o^2 - F_c^2)^2] / \sum [w(F_o^2)] \}^{1/2}.$$

program.^{40,41} The Vosko–Wilk–Nusair local density approximation⁴² with the Becke–Perdew^{43,44} generalized gradient approximations, was used for the exchange–correlation functional. The Fermi

(38) (a) Chang, C.; Pelissier, M.; Durand, P. *Phys. Scr.* **1986**, *34*, 394. (b) van Lenthe, E.; Baerends, E. J.; Snijders, J. G. *J. Chem. Phys.* **1993**, *99*, 4597. (c) van Lenthe, E.; Baerends, E. J.; Snijders, J. G. *J. Chem. Phys.* **1994**, *101*, 9783. (d) van Lenthe, E.; van Leeuwen, R.; Baerends, E. J.; Snijders, J. G. *Int. J. Quantum Chem.* **1996**, *57*, 281.

(39) (a) Dickson, R. M.; Ziegler, T. *J. Phys. Chem.* **1996**, *100*, 5286. (b) Chang, C.; Pelissier, M.; Durand, P. *Phys. Scr.* **1986**, *34*, 394.

(40) ADF 2000 02 and 2002.99, Theoretical Chemistry, Vrije Universiteit, Amsterdam, <http://www.scm.com>.

(36) Otwinowski, Z.; Minor, W. *Methods Enzymol.* **1997**, *276*, 307.

(37) Sheldrick, G. M. *SHELXTL-Windows NT, V6.12*; Bruker Analytical X-Ray Systems Inc.: Madison, WI, 2001.

contact, spin dipolar, paramagnetic spin orbit, and diamagnetic spin orbit mechanisms were included in all J_{PP} calculations; a description of these mechanisms, as implemented in the ZORA formalism, has been previously presented.⁴⁵ Triple- ζ doubly polarized ZORA-type basis sets, available with the ADF program, were employed for all atoms. Cartesian coordinates for cations **[6a]⁺** and **[8a]⁺** are available from single-crystal X-ray diffraction studies.

Preparation of $[\text{Me}_3\text{P} \cdot \text{PMe}_2=\text{NSiMe}_3]\text{Br}$ ([6a]Br**).** To a solution of **5** (0.35 g, 1.52 mmol) in 20 mL of CH_2Cl_2 was added dropwise a 1.5 mL solution of Me_3P (1.5 mmol) in toluene. The resulting thick white suspension was stirred for 2 days at ambient temperature and then allowed to settle. The supernatant was decanted and single crystals of **[6a]Br** were grown from Et_2O vapor diffusion onto the supernatant at -30°C (78.6 mg, 17%). $^{31}\text{P}\{^1\text{H}\}$ NMR (CP-MAS): 4.3 (d, $^1J_{PP} = 14$ Hz, $\text{PMe}_2=\text{N}$), 8.4 ppm (d, $^1J_{PP} = 14$ Hz, $\text{PMe}_2=\text{N}$). $^{31}\text{P}\{^1\text{H}\}$ NMR (CD_2Cl_2): -1.4 (d, $^1J_{PP} = 13.0$ Hz, $\text{PMe}_2=\text{N}$), 2.8 ppm (d, $^1J_{PP} = 12.9$ Hz, Me_3P). ^1H NMR (CD_2Cl_2): 0.16 (d, $^4J_{HP} = 0.9$ Hz, 9 H, SiMe_3), 2.10 (dd, $^2J_{HP} = 12.9$ Hz and $^3J_{HP} = 6.6$ Hz, 6 H, $\text{PMe}_2=\text{N}$), 2.45 ppm (dd, $^2J_{HP} = 6.0$ Hz and $^3J_{HP} = 0.9$ Hz, 9 H, Me_3P). $^{13}\text{C}\{^1\text{H}\}$ NMR (CD_2Cl_2): 2.5 (s, SiMe_3), 6.6 (dd, $^1J_{CP} = 40.1$ Hz and $^2J_{CP} = 2.6$ Hz, Me_3P), 20.2 ppm (dd, $^1J_{CP} = 64.1$ Hz and $^2J_{CP} = 22.0$ Hz, PMe_2).

Preparation of $[\text{Et}_3\text{P} \cdot \text{Me}_2=\text{NSiMe}_3]\text{Br}$ ([6b]Br**).** A 2 mL CDCl_3 solution of **5** (0.39 g, 1.73 mmol) was treated with a 2 mL CDCl_3 solution of Et_3P (0.20 g, 1.73 mmol) and was allowed to react for 24 h. The resulting clear and colorless solution was reduced to dryness and recrystallized from Et_2O vapor diffusion onto a saturated 4:1 $\text{CH}_3\text{CN}/\text{CHCl}_3$ solution of **[6b]Br** at -30°C (0.22 g, 37%). $^{31}\text{P}\{^1\text{H}\}$ NMR (CP-MAS): 4.4 17.8 ppm. $^{31}\text{P}\{^1\text{H}\}$ NMR (CDCl_3): 0.8 (d, $^1J_{PP} = 24.6$ Hz, $\text{PMe}_2=\text{N}$), 16.7 ppm (d, $^1J_{PP} = 24.6$ Hz, Et_3P). ^1H NMR (CDCl_3): 0.11 (d, $^4J_{HP} = 0.4$ Hz, 9 H, SiMe_3), 1.21 (d of t, $^3J_{HP} = 18.0$ Hz and $^3J_{HH} = 7.6$ Hz, 9 H, $\text{CH}_3\text{CH}_2\text{P}$), 1.96 (dd, $^2J_{HP} = 12.8$ Hz and $^3J_{HP} = 6.8$ Hz, 6 H, $\text{PMe}_2=\text{N}$), 2.55 ppm (m, 6 H, $\text{CH}_3\text{CH}_2\text{P}$). $^{13}\text{C}\{^1\text{H}\}$ NMR (CDCl_3): 2.2 (d, $^3J_{CP} = 5.9$ Hz, SiMe_3), 6.8 (dd, $^2J_{CP} = 5.9$ Hz and $^3J_{CP} = 1.1$ Hz, $\text{CH}_3\text{CH}_2\text{P}$), 11.3 (dd, $^1J_{CP} = 33.3$ Hz and $^2J_{CP} = 2.2$ Hz, $\text{CH}_3\text{CH}_2\text{P}$), 22.4 ppm (dd, $^1J_{CP} = 62.1$ Hz and $^2J_{CP} = 19.4$ Hz, $\text{PMe}_2=\text{N}$).

Preparation of $[\text{Bu}_3\text{P} \cdot \text{Me}_2=\text{NSiMe}_3]\text{Br}$ ([6c]Br**).** To a solution of **5** (1.00 g, 4.39 mmol) in 1 mL of CHCl_3 was added dropwise a 1 mL solution of $^n\text{Bu}_3\text{P}$ (0.89 g, 4.39 mmol) in CHCl_3 . The resulting colorless solution was stirred for 36 h and the volatiles were removed in vacuo to yield an adhesive white solid (1.38 g, 73%). $^{31}\text{P}\{^1\text{H}\}$ NMR (CDCl_3): -1.1 (d, $^1J_{PP} = 22.8$ Hz, $\text{PMe}_2=\text{N}$), 8.4 ppm (d, $^1J_{PP} = 22.8$ Hz, $^n\text{Bu}_3\text{P}$). ^1H NMR (CDCl_3): 0.06 (s, 9 H, SiMe_3), 0.86 (t, $^3J_{HH} = 7.2$ Hz, 9 H, CH_3), 1.36–1.57 (m, 12 H, CH_2), 2.10 (dd, $^2J_{HP} = 12.9$ Hz and $^3J_{HP} = 0.9$ Hz, 6 H, $\text{PMe}_2=\text{N}$), 2.62–2.77 ppm (m, 6 H, CH_2P). $^{13}\text{C}\{^1\text{H}\}$ NMR (CDCl_3): 3.1 (d, $^3J_{CP} = 2.9$ Hz, SiMe_3), 13.0 (s, CH_3), 17.3 (d, $^1J_{CP} = 32.1$ Hz, CH_2P), 22.1 (dd, $^1J_{CP} = 61.8$ Hz and $^2J_{CP} = 19.5$ Hz, PMe_2), 23.6 (d, $^2J_{CP} = 14.9$ Hz, CH_2), 24.0 ppm (d, $^3J_{CP} = 5.7$ Hz, CH_2).

Preparation of $[\text{Me}_2\text{PCH}_2\text{Me}_2\text{P} \cdot \text{PMe}_2=\text{NSiMe}_3]\text{Br}$ ([6d]Br**).** A 2 mL CD_2Cl_2 solution of dmpm (0.13 g, 0.95 mmol) was added quickly to a 2 mL CD_2Cl_2 solution of **5** (0.22 g, 0.95 mmol). The resulting clear and colorless solution was stirred for 18 h and then reduced to dryness which afforded a white crystalline solid. The solid was redissolved in a minimal amount of a 4:1 mixture of CH_3CN and CH_2Cl_2 , then recrystallized *via* Et_2O vapor diffusion (80.5 mg, 23%). $^{31}\text{P}\{^1\text{H}\}$ NMR (CD_2Cl_2): -47.9 (d, $^2J_{PP} = 51.6$ Hz, $\text{Me}_2\text{PCH}_2\text{Me}_2\text{P} \cdot \text{P}$), 6.7 (d, $^1J_{PP} = 17.0$ Hz, $\text{PMe}_2=\text{N}$), 10.8

ppm (dd, $^1J_{PP} = 17.1$ Hz and $^2J_{PP} = 51.3$ Hz, $\text{Me}_2\text{PCH}_2\text{Me}_2\text{P} \cdot \text{P}$). $^{13}\text{C}\{^1\text{H}\}$ NMR were complex and did not reveal useful characterization data due to coupling to inequivalent ^{31}P nuclei].

Preparation of $[\text{Me}_2\text{PCH}_2\text{CH}_2\text{Me}_2\text{P} \cdot \text{PMe}_2=\text{NSiMe}_3]\text{Br}$ ([6e]Br**).**

A CD_2Cl_2 solution (2 mL) of dmpm (0.24 g, 1.63 mmol) was combined with a rapidly stirring CD_2Cl_2 solution of **5** (0.37 g, 1.63 mmol) and allowed to react for 18 h. The resulting white suspension was allowed to settle and the supernatant decanted. A white crystalline solid was obtained after all volatiles were removed from the supernatant and then recrystallized from a saturated solution of **[6d]Br** in a 4:1 mixture of CH_3CN and CHCl_3 (0.11 g, 18%). $^{31}\text{P}\{^1\text{H}\}$ NMR (CP-MAS): -46.2 (d, $^3J_{PP} = 32$ Hz, $\text{Me}_2\text{PCH}_2\text{CH}_2\text{Me}_2\text{P} \cdot \text{P}$), -4.1 (d, $^1J_{PP} = 22$ Hz, $\text{PMe}_2=\text{N}$), 8.9 ppm (dd, $^1J_{PP} = 22$ Hz and $^3J_{PP} = 32$ Hz, $\text{Me}_2\text{PCH}_2\text{CH}_2\text{Me}_2\text{P} \cdot \text{P}$). $^{31}\text{P}\{^1\text{H}\}$ NMR (CD_2Cl_2): -42.5 (d, $^3J_{PP} = 25.1$ Hz, $\text{Me}_2\text{PCH}_2\text{CH}_2\text{Me}_2\text{P} \cdot \text{P}$), 3.3 (d, $^1J_{PP} = 20.2$ Hz, $\text{PMe}_2=\text{N}$), 9.1 ppm (dd, $^1J_{PP} = 20.2$ Hz and $^3J_{PP} = 31.4$ Hz, $\text{Me}_2\text{PCH}_2\text{CH}_2\text{Me}_2\text{P} \cdot \text{P}$). ^1H and $^{13}\text{C}\{^1\text{H}\}$ NMR were complex and did not reveal useful characterization data due to coupling to inequivalent ^{31}P nuclei].

Preparation of $[\text{Me}_3\text{P} \cdot \text{P}(\text{CF}_3\text{CH}_2\text{O})_2=\text{NSiMe}_3]\text{Br}$ ([8a]Br**).** To a solution of **7** (0.46 g, 1.17 mmol) in 5 mL of CHCl_3 was added dropwise a 1.2 mL solution of Me_3P (1.2 mmol) in toluene. The resulting white suspension was stirred for 24 h and the volatiles were removed in vacuo and yielded a crystalline white solid (0.48 g, 87%). Crystals of **[8a]Br** were grown *via* Et_2O vapor diffusion onto a saturated CHCl_3 solution of **[8a]Br** at -30°C . $^{31}\text{P}\{^1\text{H}\}$ NMR (CP-MAS): -16.4 (d, $^1J_{PP} = 322$ Hz, $\text{P}(\text{OCH}_2\text{CF}_3)_2=\text{N}$), 11.1 ppm (d, $^1J_{PP} = 322$ Hz, Me_3P). $^{31}\text{P}\{^1\text{H}\}$ NMR (CDCl_3): -15.6 (d, $^1J_{PP} = 324.0$ Hz, $\text{P}(\text{OCH}_2\text{CF}_3)_2=\text{N}$), 11.9 ppm (d, $^1J_{PP} = 323.8$ Hz, Me_3P). ^1H NMR (CDCl_3): 0.09 (d, $^4J_{HP} = 0.3$ Hz, 9H, SiMe_3), 2.47 (dd, $^2J_{HP} = 14.8$ Hz and $^3J_{HP} = 11.2$ Hz, 9 H, Me_3P), 4.61 ppm (d of m, 4 H, OCH_2CF_3). $^{13}\text{C}\{^1\text{H}\}$ (CDCl_3): 2.8 (s, SiMe_3), 7.4 (dd, $^1J_{CP} = 44.1$ Hz and $^2J_{CP} = 4.8$ Hz, Me_3P), 63.4 (q of d, $^2J_{CF} = 38.1$ Hz and $^2J_{CP} = 4.9$ Hz, OCH_2CF_3), 122.4 ppm (q of d, $^1J_{CF} = 278.2$ Hz and $^3J_{CP} = 8.3$ Hz, OCH_2CF_3). ^{19}F (CDCl_3): -74.7 ppm (t, $^3J_{FH} = 8.5$ Hz).

Preparation of $[\text{Et}_3\text{P} \cdot \text{P}(\text{CF}_3\text{CH}_2\text{O})_2=\text{NSiMe}_3]\text{Br}$ ([8b]Br**).** A solution of **7** (0.44 g, 1.12 mmol) in 3 mL of CHCl_3 was treated with a solution Et_3P (0.13 g, 1.12 mmol) in 3 mL of CHCl_3 and stirred for 18 h. The clear, colorless solution was reduced to dryness which afforded a crystalline white solid (0.38 g, 67%). Crystals of **[8b]Br** were grown from Et_2O vapor diffusion onto a saturated CHCl_3 solution of **[8b]Br** at -30°C . $^{31}\text{P}\{^1\text{H}\}$ NMR (CP-MAS): -8.6 (d, $^1J_{PP} = 262$ Hz, $\text{P}(\text{OCH}_2\text{CF}_3)_2=\text{N}$), 26.6 ppm (d, $^1J_{PP} = 262$ Hz, Et_3P). $^{31}\text{P}\{^1\text{H}\}$ NMR (CDCl_3): -19.3 (d, $^1J_{PP} = 276.0$ Hz, $\text{P}(\text{OCH}_2\text{CF}_3)_2=\text{N}$), 27.5 ppm (d, $^1J_{PP} = 276.1$ Hz, Et_3P). ^1H NMR (CDCl_3): 0.17 (d, $^4J_{HP} = 0.9$ Hz, 9 H, SiMe_3), 1.40 (dtd, $^3J_{HH} = 7.5$ Hz, $^3J_{HP} = 19.8$ Hz, $^4J_{HP} = 0.9$ Hz, 9 H, $\text{CH}_3\text{CH}_2\text{P}$), 2.86–3.02 (m, 6 H, $\text{CH}_3\text{CH}_2\text{P}$), 4.48–4.91 ppm (m, 4 H, OCH_2CF_3). $^{13}\text{C}\{^1\text{H}\}$ NMR (CDCl_3): 2.7 (d, $^3J_{CP} = 2.6$ Hz, SiMe_3), 6.5 (d, $^2J_{CP} = 6.0$ Hz, $\text{CH}_3\text{CH}_2\text{P}$), 12.8 (dd, $^1J_{CP} = 37.0$ Hz and $^2J_{CP} = 4.6$ Hz, $\text{CH}_3\text{CH}_2\text{P}$), 63.1 (q of q, $^2J_{CF} = 38.1$ Hz and $^2J_{CP} = 9.1$ Hz, OCH_2CF_3), 122.3 ppm (q of d, $^1J_{CF} = 277.8$ Hz and $^3J_{CP} = 8.3$ Hz, OCH_2CF_3). ^{19}F (CDCl_3): -74.6 ppm (t, $^3J_{FH} = 8.5$ Hz).

Preparation of $[\text{Bu}_3\text{P} \cdot \text{P}(\text{CF}_3\text{CH}_2\text{O})_2=\text{NSiMe}_3]\text{Br}$ ([8c]Br**).**

To a solution of **7** (1.16 g, 2.93 mmol) in 1 mL of CHCl_3 was added dropwise a 1 mL solution of $^n\text{Bu}_3\text{P}$ (0.59 g, 2.93 mmol) in CHCl_3 . The resulting colorless solution was stirred for 24 h and the volatiles were removed in vacuo and yielded a clear and colorless oil (1.68 g, 96%). $^{31}\text{P}\{^1\text{H}\}$ NMR (CDCl_3): -18.5 (d, $^1J_{PP} = 277.9$ Hz, $\text{P}(\text{OCH}_2\text{CF}_3)_2=\text{N}$), 22.2 ppm (d, $^1J_{PP} = 277.3$ Hz, $^n\text{Bu}_3\text{P}$). ^1H NMR (CDCl_3): 0.06 (s, 9 H, SiMe_3), 0.85 (t, $^3J_{HH} = 7.2$ Hz, 9 H, CH_3), 1.36–1.57 (m, 12 H, CH_2), 2.62–2.77 (m, 6 H, CH_2P), 4.58–4.78 ppm (m, 4 H, OCH_2CF_3). $^{13}\text{C}\{^1\text{H}\}$ NMR (CDCl_3): 2.4 (d, $^3J_{CP} = 2.3$ Hz, SiMe_3), 13.2 (s, CH_3), 18.8 (dd, $^1J_{CP} = 35.5$ Hz and $^2J_{CP} = 4.5$ Hz, CH_2P), 23.6 (s, CH_2), 23.8 (s, CH_2), 63.0 (q of d, $^2J_{CF} = 37.5$ Hz and $^2J_{CP} = 8.0$ Hz, OCH_2CF_3), 122.3 ppm (q of d, $^1J_{CF} = 277.7$ Hz and $^3J_{CP} = 8.9$ Hz, OCH_2CF_3). ^{19}F NMR (CDCl_3): -74.7 ppm (t, $^3J_{FH} = 7.6$ Hz).

- (41) (a) Baerends, E. J.; Ellis, D. E.; Ros, P. *Chem. Phys.* **1973**, *2*, 41. (b) Versluis, L.; Ziegler, T. *J. Chem. Phys.* **1988**, *88*, 322. (c) te Velde, G.; Baerends, E. J. *J. Comput. Phys.* **1992**, *99*, 84. (d) Fonseca Guerra, C.; Snijders, J. G.; te Velde, G.; Baerends, E. J. *Theor. Chem. Acc.* **1998**, *99*, 391.
 (42) Vosko, S. H.; Wilk, L.; Nusair, M. *Can. J. Phys.* **1980**, *58*, 1200.
 (43) Becke, A. D. *Phys. Rev. A* **1988**, *38*, 3098.
 (44) Perdew, J. P. *Phys. Rev. B* **1986**, *33*, 8822; **1986**, *34*, 7406.
 (45) Autschbach, J.; Ziegler, T. *J. Chem. Phys.* **2000**, *113*, 936.

Preparation of [Me₂PCH₂Me₂P·P(CF₃CH₂O)₂]=NSiMe₃]Br ([8d]Br). A 2 mL CD₂Cl₂ solution of dmpm (0.16 g, 1.15 mmol) was added to a CD₂Cl₂ solution of **7** (0.46 g, 1.15 mmol) and stirred for 4 h. All volatiles were removed from the reaction solution which yielded a white crystalline solid. The solid was recrystallized from Et₂O vapor diffusion onto a saturated solution [8d]Br in a 4:1 mixture of CH₃CN/CHCl₃ (0.45 g, 73%). ³¹P{¹H} NMR (CD₂Cl₂): -49.1 (d, ²J_{PP} = 63.6 Hz, Me₂PCH₂Me₂P), -15.2 (d, ¹J_{PP} = 316.2 Hz, PMe₂=N), 16.9 ppm (dd, ¹J_{PP} = 316.2 Hz and ²J_{PP} = 63.4 Hz, Me₂PCH₂Me₂P·P). ¹H NMR (CD₂Cl₂): δ = 0.06 (s, 9 H, SiMe₃), 1.24 (d, ²J_{HP} = 3.6 Hz, 6 H, Me₂PCH₂Me₂P·P), 2.35 (dd, ²J_{HP} = 14.4 Hz and ³J_{HP} = 11.2 Hz, 6 H, Me₂PCH₂Me₂P·P), 3.12 (dd, ²J_{HP} = 15.6 Hz and ²J_{HP} = 13.2 Hz, 2 H, Me₂PCH₂Me₂P·P), 4.66 ppm (m, 4 H, OCH₂CF₃). ¹³C{¹H} NMR (CD₂Cl₂): 2.7 (d, ³J_{CP} = 3.0 Hz, SiMe₃), 7.7 (d of t, ¹J_{CP} = 44.5 Hz and ²J_{CP} = 5.2 Hz, Me₂PCH₂Me₂P·P), 15.9 (dd, ¹J_{CP} = 13.5 Hz and ²J_{CP} = 8.9 Hz, Me₂PCH₂Me₂P·P), 22.3 (m, Me₂PCH₂Me₂P·P), 63.9 (m, OCH₂CF₃), 122.9 ppm (d of q, ¹J_{CF} = 277.5 Hz and ³J_{CP} = 7.4 Hz, OCH₂CF₃).

Preparation of [Me₂PCH₂CH₂Me₂P·P(CF₃CH₂O)₂]=NSiMe₃]Br ([8e]Br). A 5 mL CD₂Cl₂ solution **7** (0.37 g, 0.93 mmol) was treated with dmpe (0.24 g, 1.63 mmol) in 3 mL of CD₂Cl₂. The reaction solution was stirred for 36 h and then reduced to dryness which afforded a white crystalline solid (0.57 g, 98%). ³¹P{¹H} NMR (CDCl₃): -42.6 (d, ³J_{PP} = 33.8 Hz, Me₂PCH₂CH₂P·P), -15.1 (d, ¹J_{PP} = 302.4 Hz, P(OCH₂CF₃)₂=N), 18.1 ppm (dd, ¹J_{PP} = 302.4 Hz and ³J_{PP} = 35.8 Hz, Me₂PCH₂CH₂P·P). ¹H NMR (CD₂Cl₂): δ = 0.06 (s, 9 H, SiMe₃), 1.01 (s (br), 6 H, Me₂PCH₂CH₂Me₂P·P), 1.59 (s (br), 2 H, Me₂PCH₂CH₂Me₂P·P), 2.41 (t (br), ¹J_{HP} = 12.4 Hz, 2 H, Me₂PCH₂CH₂Me₂P·P), 2.95 (s (br), 6 H, Me₂PCH₂CH₂Me₂P·P), 4.18 ppm (d of m (br), ¹J_{HP} = 151.5 Hz, 4 H, OCH₂CF₃). ¹³C{¹H} NMR (CD₂Cl₂): 2.8 (d, ³J_{CP} = 2.3 Hz, SiMe₃), 6.3 (dd, ¹J_{CP} = 43.0 Hz and ²J_{CP} = 5.2 Hz, Me₂PCH₂CH₂Me₂P·P), 13.5 (d, ¹J_{CP} = 13.9 Hz, Me₂PCH₂CH₂Me₂P·P), 19.2 (m, ¹J_{CP} = 17.5 Hz and ²J_{CP} = 3.7 Hz, Me₂PCH₂CH₂Me₂P·P), 23.2 (dd, ¹J_{CP} = 16.8 Hz and ²J_{CP} = 7.1 Hz, Me₂PCH₂CH₂Me₂P·P), 63.8 (m, OCH₂CF₃), 122.9 ppm (d of q, ¹J_{CF} = 277.8 Hz and ³J_{CP} = 7.1 Hz, OCH₂CF₃).

Preparation of [Me₂PhP·P(CF₃CH₂O)₂]=NSiMe₃]Br ([8f]Br). To a solution of **7** (0.35 g, 0.88 mmol) in 5 mL of CH₂Cl₂ was added a solution of Me₂PhP (0.12 g, 0.88 mmol). The reaction suspension was stirred for 36 h and then analyzed by ³¹P{¹H} NMR spectroscopy which revealed ca. 20% conversion of the substrates to [8f]Br. Continued stirring of the white suspension resulted in the formation of a number of unidentified products. Data for [8f]Br: ³¹P{¹H} NMR (CH₂Cl₂): -19.3 (d, ¹J_{PP} = 329.8 Hz, P(OCH₂CF₃)₂=N), 4.8 ppm (d, ¹J_{PP} = 329.7 Hz, Me₂PhP).

Reaction between [6a]Br and DMAP: Preparation of [DMAP·PMe₂=NSiMe₃]Br ([9]Br). A 3 mL CHCl₃ solution of DMAP (0.54 g, 4.39 mmol) was added to a solution of [6a]Br, prepared in situ from **5** (1.00 g, 4.39 mmol) and ⁿBu₃P (0.89 g, 4.39 mmol) in 1 mL of CHCl₃. After stirring for 1.5 h the clear, colorless solution was analyzed by ³¹P{¹H} NMR spectroscopy which indicated the complete conversion of [6a]Br to the DMAP-stabilized phosphoranime salt [9]Br and the presence of ⁿBu₃P [³¹P{¹H} NMR (CHCl₃): -31.3 (s, ⁿBu₃P, ca. 51%), 25.3 ppm (s, [9]⁺, ca. 49%)]. The reaction solution was reduced to dryness and the crude product was purified via a slow vapor diffusion of Et₂O onto a saturated CH₃CN solution where clear and colorless crystals of [9]Br, suitable for a single crystal X-ray diffraction study, were grown (1.41 g, 92%). ³¹P{¹H} NMR (CDCl₃): 27.4 ppm (s). ¹H NMR (CDCl₃): 0.05 (d, ⁴J_{HP} = 0.6 Hz, 9H, SiMe₃), 2.15 (d, ²J_{HP} = 13.8 Hz, 6H, P-Me), 3.29 (s, 6H, NMe₂), 6.95 (d, ¹J = 7.8 Hz, 2H, ArH), 9.17 ppm (t, ¹J = 8.1 Hz, 2H, ArH). ¹³C{¹H} NMR (CDCl₃): 3.5 (d, ²J_{CP} = 4.9 Hz, SiMe₃), 21.0 (d, ¹J_{CP} = 79.6 Hz, P-Me), 40.9 (s, NMe₂), 108.0 (d, ³J_{CP} = 3.5 Hz, *m*-C), 141.2 (d, ³J_{CP} = 6.0 Hz, *o*-C), 157.5 (s, *p*-C). Anal. Calcd for C₁₂H₂₅N₃PSiBr (350.31): C, 41.14; H, 7.70; N, 11.99. Found: C, 40.16; H, 6.86; N, 12.25.

Reaction between [8c]Br and DMAP: Preparation of [DMAP·P(CF₃CH₂O)₂]=NSiMe₃]Br ([10]Br). A 3 mL CHCl₃ solution of DMAP (0.36 g, 2.93 mmol) was added to a solution of [8c]Br, prepared in situ from **7** (1.16 g, 2.93 mmol) and ⁿBu₃P (0.59 g, 2.93 mmol) in 1 mL of CHCl₃. After stirring for 1.5 h the clear, colorless solution was analyzed by ³¹P{¹H} NMR spectroscopy which indicated the complete conversion of [8c]Br to the DMAP-stabilized phosphoranime salt [10]Br and the presence of ⁿBu₃P. ³¹P{¹H} NMR (CDCl₃): -31.7 (s, ⁿBu₃P, ca. 49%), -22.4 ppm (s, [11]⁺, ca. 51%). All volatiles were removed which yielded a white crystalline solid (1.40 g, 92%). ³¹P{¹H} NMR (CDCl₃): -22.4 ppm (s). ¹H NMR (CDCl₃): 0.18 (s, 9H, SiMe₃), 3.48 (s, 6H, NMe₂), 4.53 (q of d, ³J_{HF} = 12.0 Hz and ³J_{HP} = 7.8 Hz, 4H, OCH₂CF₃), 7.28 (dd, ¹J_{HH} = 2.4 and 8.4 Hz, 2H, *m*-ArH), 8.24 ppm (t, ¹J_{HH} = 8.1 Hz, 2H, *o*-ArH). ¹³C{¹H} NMR (CDCl₃): 2.4 (d, ³J_{CP} = 3.5 Hz, SiMe₃), 41.6 (s, NMe₂), 64.3 (q of d, ²J_{CF} = 38.1 Hz and ²J_{CP} = 4.9 Hz, OCH₂CF₃), 108.9 (d, ²J_{CP} = 8.0 Hz, *o*-C), 121.9 (q of d, ¹J_{CF} = 278.2 Hz and ³J_{CP} = 8.3 Hz, OCH₂CF₃), 140.0 (d, ³J_{CP} = 5.7 Hz, *m*-C), 157.5 ppm (s, *p*-C). ¹⁹F NMR (CDCl₃): -74.7 ppm (t, ³J_{FF} = 8.5 Hz, OCH₂CF₃). Anal. Calcd for C₁₄H₂₃F₆BrN₃O₂PSi (518.3): C, 32.44; H, 4.47; N, 8.11. Found: C, 32.84; H, 4.43; N, 8.20.

Preparation of [Et₃P·PMe₂=NSiMe₃]OTf ([6b]OTf). The salt [6b]Br was prepared in situ from the treatment of a 3 mL CH₂Cl₂ solution of **5** (0.25 g, 1.10 mmol) with a 1 mL CH₂Cl₂ solution of Et₃P (0.13 g, 1.10 mmol). After stirring overnight, the resulting solution was added to a stirred suspension of AgOTf (0.28 g, 1.10 mmol) and allowed to react for 3 h. The white suspension was filtered and reduced to dryness. The resulting white solid was recrystallized from CH₂Cl₂ via Et₂O vapor diffusion (83 mg, 18%). ³¹P{¹H} NMR (CDCl₃): 0.8 (d, ¹J_{PP} = 24.6 Hz, PMe₂=N), 16.7 ppm (d, ¹J_{PP} = 24.6 Hz, Et₃P). ¹H NMR (CDCl₃): 0.11 (d, ⁴J_{HP} = 0.4 Hz, 9 H, SiMe₃), 1.21 (d of t, ³J_{HP} = 18.0 Hz and ³J_{HH} = 7.6 Hz, 9 H, CH₃CH₂P), 1.96 (dd, ²J_{HP} = 12.8 Hz and ³J_{HP} = 6.8 Hz, 6 H, PMe₂=N), 2.55 ppm (m, 6 H, CH₃CH₂P). ¹³C{¹H} NMR (CDCl₃): 2.2 (d, ³J_{CP} = 5.9 Hz, SiMe₃), 6.8 (dd, ²J_{CP} = 5.9 Hz and ³J_{CP} = 1.1 Hz, CH₃CH₂P), 11.3 (dd, ¹J_{CP} = 33.3 Hz and ²J_{CP} = 2.2 Hz, CH₃CH₂P), 22.4 (dd, ¹J_{CP} = 62.1 Hz and ²J_{CP} = 19.4 Hz, PMe₂=N), 120.7 ppm (q, ¹J_{CF} = 320.1 Hz, OTf). ¹⁹F NMR (CDCl₃): -78.4 ppm (s, OTf).

Preparation of [ⁿBu₃P·P(CF₃CH₂O)₂]=NSiMe₃]OTf ([8c]OTf). The salt [8c]Br was prepared in situ from the direct reaction between **7** (0.33 g, 0.83 mmol) and ⁿBu₃P (0.17 g, 0.83 mmol) in 3 mL of CHCl₃ and stirred for 18 h. The resulting reaction solution was diluted with 3 mL of CHCl₃ and added rapidly to a stirred suspension of AgOTf (0.21 g, 0.83 mmol) in the absence of light. The white suspension was stirred for an additional 12 h and then filtered. All volatiles were removed from the filtrate which afforded the salt [8c]OTf as a viscous oil (0.17 g, 32%). ³¹P{¹H} NMR (CDCl₃): -19.3 (d, ¹J_{PP} = 284.5 Hz), 21.8 ppm (d, ¹J_{PP} = 284.5 Hz). ¹H NMR (CDCl₃): 0.18 (s, 9 H, SiMe₃), 0.98 (t, ³J_{HH} = 7.2 Hz, 9 H, CH₃), 1.47–1.66 (m, 12 H, CH₂), 2.38–2.53 (m, 6 H, CH₂P), 4.55–4.72 ppm (m, 4 H, OCH₂CF₃). ¹³C{¹H} NMR (CDCl₃): 2.6 (d, ³J_{CP} = 2.3 Hz, SiMe₃), 13.3 (s, CH₃), 18.5 (dd, ¹J_{CP} = 35.8 Hz and ²J_{CP} = 4.9 Hz, CH₂P), 23.8 (s, CH₂), 24.1 (s, CH₂), 62.9 (q of d, ²J_{CF} = 39.2 Hz and ²J_{CP} = 8.8 Hz, OCH₂CF₃), 120.7 (q, ¹J_{CF} = 320.1 Hz, OTf), 122.4 ppm (q of d, ¹J_{CF} = 277.7 Hz and ³J_{CP} = 8.8 Hz, OCH₂CF₃). ¹⁹F NMR (CDCl₃): -78.4 (s, OTf), -74.8 ppm (t, ³J_{FF} = 7.6 Hz, OCH₂CF₃).

Reaction between [6b]Br and B(C₆F₅)₃. The salt [6b]Br was prepared in situ from the treatment of a 3 mL CHCl₃ solution of **5** (0.33 g, 1.45 mmol) with a 1 mL CHCl₃ solution of Et₃P (0.17 g, 1.45 mmol). After stirring the solution for 18 h a 5 mL CHCl₃ solution of B(C₆F₅)₃ (0.74 g, 1.45 mmol) was added to the reaction mixture and stirred for 36 h and then analyzed by ³¹P{¹H} NMR spectroscopy, which indicated the complete retroconversion of [6b]Br to **5** and Et₃P·B(C₆F₅)₃ [³¹P{¹H}: 4.5 ppm (br d, ¹J_{PB} = 85.3 Hz). ¹¹B{¹H}: -13.6 ppm (br d, ¹J_{BP} = 68.6 Hz)].

Reaction between [8c]Br and B(C₆F₅)₃. To a solution of [8c]Br, prepared in situ from **7** (0.36 g, 0.91 mmol) and ¹⁰Bu₃P (0.18 g, 0.91 mmol), in 5 mL of CHCl₃ was added a suspension of B(C₆F₅)₃ (0.47 g, 0.91 mmol) in CHCl₃. The reaction solution was stirred for 36 h and then analyzed by ³¹P{¹H} NMR spectroscopy, indicating the full retroconversion of [8c]Br to **7** (−34.2 ppm) and the production of ⁿBu₃P·B(C₆F₅)₃ [³¹P{¹H}: 0.2 ppm (br). ¹¹B{¹H}: −13.4 ppm (br)].

Decomposition of [6a]Br. A CDCl₃ solution derived from single crystals of [6a]Br was allowed to stand, undisturbed, in an NMR tube under N₂. After 7 days, single crystals of [Me₂P=N]₄ (**13**) grew within the NMR tube and were analyzed by X-ray crystallography. The mother liquor was analyzed by ³¹P{¹H} NMR which indicated the presence of [Me₂P=N]₃ (34.2 ppm), [Me₂P=N]₄ (27.1 ppm), and [Me₃P=N]₅ (22.3 ppm). The presence of BrSiMe₃ (0.64 ppm) was also detected by ¹H NMR. The mother liquor was then reduced to dryness and the resulting white solid was analyzed by electron impact mass spectrometry which indicated the presence of [Me₂P=N]₆ and [Me₂P=N]₇. EI-MS (70 eV, *m/z*, %): 525 ([Me₂P=N]₇)⁺, 450 ([Me₂P=N]₆)⁺, 23), 375 ([Me₂P=N]₅)⁺, 22), 301 ([Me₂P=N]₄ + H)⁺, 23), 300 ([Me₂P=N]₄)⁺, 16), 285 ([Me₂P=N]₄ − Me)⁺, 75), 210 ([Me₂P=N]₃ − Me)⁺, 86), 147 ([Me₂PNSiMe₃)⁺, 100).

Solution Decomposition of [6b]Br. Crystals of [6b]Br were dissolved in CDCl₃ (25 mg/mL) and analyzed by ³¹P{¹H} NMR after 10 min showing 96% retroconversion to BrPMe₂=NSiMe₃ and PEt₃: −18.0 (s), 0.8 (d, ¹J_{PP} = 24.6 Hz), 10.0 (s), and 16.7 ppm (d, ¹J_{PP} = 24.6 Hz). No further change was observed after the solution was allowed to stand at room temperature for 5 days.

Thermal Decomposition of [8b]Br. A CDCl₃ solution of [8b]Br (25 mg/mL) was allowed to stand at room temperature for 24 h and was then analyzed by ³¹P{¹H} NMR: δ = −33.5 (s, BrP(OCH₂CF₃)₂=NSiMe₃), −19.3 (d, ¹J_{PP} = 276.0 Hz), −18.0 (s, Et₃P), 27.5 ppm (d, ¹J_{PP} = 276.0 Hz). After standing for 2 and 5 d integrals of the peaks (relative to the total integral of all peaks) at −33.5 and −18.0 ppm showed the conversion to be 7% and 11% respectively. In a separate experiment, a CDCl₃ solution of [8b]Br was heated in a J Young NMR tube at 100 °C for 3 days which resulted in the precipitation of a white solid coupled with a yellow solution. After filtration, both the solid and filtrate were analyzed.

Data for filtrate: ³¹P{¹H} NMR (CDCl₃): δ = 4.5 (d, ¹J_{PP} = 14.2 Hz), 42.1 (d, ¹J_{PP} = 21.4 Hz), 43.4 (d, ¹J_{PP} = 14.7 Hz), 43.7 (d, ¹J_{PP} = 11.5 Hz), 43.8 (d, ¹J_{PP} = 11.5 Hz), and 87.3 (d, ¹J_{PP} = 21.0 Hz).

Thermal Decomposition of [6b]OTf. A CDCl₃ solution of [6b]OTf was allowed to stand at room temperature for 7 days, after which no decomposition was observable by ³¹P{¹H} NMR: 0.8 (d, ¹J_{PP} = 24.6 Hz), 16.7 ppm (d, ¹J_{PP} = 24.6 Hz). Heating the solution to 100 °C in a sealed tube for 1 d resulted in complete decomposition by ³¹P{¹H} NMR: −17.4 (br), 26.2 (br), 43.4 (s), 43.9 (s), 62.4 ppm (s). A small quantity of an insoluble oil was also observed.

Preparation and Thermal Decomposition of [Et₃P·P(CF₃CH₂O)₂=NSiMe₃]OTf ([8b]OTf). A 1 mL CH₂Cl₂ suspension of [8b]Br (103 mg, 0.20 mmol) and AgOTf (51 mg, 0.2 mmol) was stirred for 3 min then filtered. An oil was precipitated from the filtrate via Et₂O vapor diffusion and the supernatant analyzed by ³¹P{¹H} NMR: −17.6 (d, ¹J_{PP} = 282 Hz), 28.8 ppm (d, ¹J_{PP} = 282 Hz). No change was observed by NMR after the solution was kept at room temperature for 6 days. Heating the solution to 100 °C in a sealed tube for 1 day resulted in partial decomposition of [8b]OTf by ³¹P{¹H} NMR: −17.5 (d, ¹J_{PP} = 281 Hz), −16.7 (s), −10.9 (d, ¹J_{PP} = 23 Hz), −8.6 (s), 29.0 (d, ¹J_{PP} = 23 Hz), 41.1 (s), 49.8 (d, ¹J_{PP} = 281 Hz), 93.8 ppm (s). A small quantity of insoluble solid was also observed.

Acknowledgment. This research was supported by the Natural Sciences and Engineering Research Council of Canada (NSERC) and the European Union (E.U.). K.H. thanks NSERC for a Postgraduate Fellowship (2005–2008), A.P. thanks the E.U. for a Marie Curie Postdoctoral Fellowship, and I.M. would like to thank the Canadian Government for a Canada Research Chair at Toronto, the E.U. for Marie Curie Chair and the Royal Society for a Wolfson Research Merit Award at Bristol. REW acknowledges the Government of Canada for a Canada Research Chair in physical chemistry.

Supporting Information Available: Crystallographic information (cif) files and detailed structural data (pdf). This material is available free of charge via the Internet at <http://pubs.acs.org>.

JA900256G